

ORIGINAL ARTICLE

DNA Methylation-Mediated Modulation of Endocytosis as Potential Mechanism for Synaptic Function Regulation in Murine Inhibitory Cortical Interneurons

Daniel Pensold^{1,2}, Julia Reichard^{1,2,3}, Karen M. J. Van Loo⁴, Natalja Ciganok⁵, Anne Hahn¹, Cathrin Bayer^{1,2}, Lutz Liebmann¹, Jonas Groß¹, Jessica Tittelmeier¹, Thomas Lingner⁶, Gabriela Salinas-Riester⁶, Judit Symmank¹, Claas Halfmann⁵, Lourdes González-Bermúdez¹, Anja Urbach⁷, Julia Gehrman⁸, Ivan Costa⁸, Tomas Pieler⁹, Christian A. Hübner¹, Hartmut Vatter¹⁰, Björn Kampa^{5,11}, Albert J. Becker⁴ and Geraldine Zimmer-Bensch^{1,2,3}

¹Institute of Human Genetics, University Hospital Jena, 07743 Jena, Germany, ²Division of Functional Epigenetics, Institute of Zoology (Biology 2), RWTH Aachen University, 52074 Aachen, Germany, ³Research Training Group 2416 Multi Senses–Multi Scales, RWTH Aachen University, 52074 Aachen, Germany, ⁴Department of Neuropathology, Section for Translational Epilepsy Research, University of Bonn Medical Center, 53105 Bonn, Germany, ⁵Division of Systems Neurophysiology, Institute of Zoology (Biology 2), RWTH Aachen University, 52074 Aachen, Germany, ⁶Department of Developmental Biochemistry, Transcriptome and Genome Analysis Laboratory (TAL), University of Goettingen, 37077 Goettingen, Germany, ⁷Clinic for Neurology, University Hospital Jena, 07743 Jena, Germany, ⁸Institute for Computational Genomics, University Hospital Aachen, RWTH Aachen University, 52074 Aachen, Germany, ⁹Department of Developmental Biochemistry, Centre for Nanoscale Microscopy and Molecular Physiology of the Brain (CNMPB), University of Goettingen, 37077 Goettingen, Germany, ¹⁰Clinic for Neurosurgery, University of Bonn Medical Center, 53105 Bonn, Germany and ¹¹JARA BRAIN, Institute for Neuroscience and Medicine, Forschungszentrum Jülich, 52425, Germany

Address correspondence to Geraldine Zimmer-Bensch, Division of Functional Epigenetics, Institute of Zoology, RWTH Aachen University, Worringerweg 3, 52074 Aachen, Germany. Email: zimmer_geraldine@yahoo.de

Daniel Pensold, Julia Reichard, Karen M. J. Van Loo and Natalja Ciganok have contributed equally to this work.

Abstract

The balance of excitation and inhibition is essential for cortical information processing, relying on the tight orchestration of the underlying subcellular processes. Dynamic transcriptional control by DNA methylation, catalyzed by DNA methyltransferases (DNMTs), and DNA demethylation, achieved by ten–eleven translocation (TET)-dependent mechanisms, is proposed to regulate synaptic function in the adult brain with implications for learning and memory. However, focus so far is laid on excitatory neurons. Given the crucial role of inhibitory cortical interneurons in cortical information processing and in disease, deciphering the cellular and molecular mechanisms of GABAergic transmission is fundamental. The

© The Author(s) 2020. Published by Oxford University Press.

This is an Open Access article distributed under the terms of the Creative Commons Attribution Non-Commercial License (<http://creativecommons.org/licenses/by-nc/4.0/>), which permits non-commercial re-use, distribution, and reproduction in any medium, provided the original work is properly cited. For commercial re-use, please contact journals.permissions@oup.com

emerging relevance of DNMT and TET-mediated functions for synaptic regulation irrevocably raises the question for the targeted subcellular processes and mechanisms. In this study, we analyzed the role dynamic DNA methylation has in regulating cortical interneuron function. We found that DNMT1 and TET1/TET3 contrarily modulate clathrin-mediated endocytosis. Moreover, we provide evidence that DNMT1 influences synaptic vesicle replenishment and GABAergic transmission, presumably through the DNA methylation-dependent transcriptional control over endocytosis-related genes. The relevance of our findings is supported by human brain sample analysis, pointing to a potential implication of DNA methylation-dependent endocytosis regulation in the pathophysiology of temporal lobe epilepsy, a disease characterized by disturbed synaptic transmission.

Key words: cortical inhibition, DNMT1, GABA, synaptic function, temporal lobe epilepsy, TET

Introduction

In the mammalian cortex, the seat of higher brain functions, neuronal information processing critically depends on inhibitory gamma-aminobutyric acid (GABA)-positive interneurons, actively shaping the responses of excitatory glutamatergic principal neurons (Hensch 2005; Letzkus et al. 2015). Timed inhibition is crucial for the generation of network oscillations underlying the coordination of communication between different brain areas (Fries 2009; Buzsaki and Wang 2012). Moreover, increasing evidence for a timed and local disinhibition emerges as a critical mechanism for learning and memory formation (Letzkus et al. 2015).

The molecular basis for learning and memory relies on synaptic plasticity, which is modulated by action potential-dependent and spontaneous transmitter release, influencing the strength of synaptic connections. Both processes are subject to modulation requiring multiple levels of regulation for efficient management (Bouron 2001).

Several studies have highlighted the relevance of protein turnover, including their removal from the cell surface, recycling, or degradation for synaptic function and plasticity (Cajigas et al. 2010). These processes rely on clathrin- and dynamin-dependent endocytosis (Malinow and Malenka 2002; Brecht and Nicoll 2003; Turrigiano 2008). Although several different types of endocytosis exist (Huotari and Helenius 2011), clathrin-mediated endocytosis is crucially implicated in the internalization of receptors required for neuronal signaling (Parton and Dotti 1993; Cosker and Segal 2014). After the internalization of cargo, the endocytic vesicle can fuse with early endosomes and is either recycled back via recycling endosomes or degraded after their maturation to late endosomes and the fusion with lysosomes (Huotari and Helenius 2011). At synapses, endocytic-based recycling is implicated in synaptic vesicle replenishment, thereby influencing synaptic transmission (Kuromi and Kidokoro 2005). The efficient management of synaptic transmission and its underlying processes require multiple levels of regulation.

It is becoming increasingly clear that epigenetic mechanisms of gene regulation, including histone modifications and DNA methylation, are critically involved in processes underlying learning and memory (Meadows et al. 2016; Sweatt 2017), albeit the detailed subcellular mechanisms remain largely unknown. In excitatory neurons of the cerebral cortex, a role of DNA methyltransferases (DNMTs), the enzymes that catalyze 5-cytosine methylation, in modulating synaptic transmission (Levenson et al. 2006; Nelson et al. 2008; Sweatt 2016), synaptic scaling (Meadows et al. 2015), and neuronal excitability (Meadows et al. 2016) was already reported.

In support of its relevance for synaptic functionality, DNA methylation has emerged as a highly dynamic process in developing and mature neurons (Guo et al. 2011a, 2011b, 2014).

This is enabled by active ways of DNA demethylation, involving ten-eleven translocation (TET) family enzyme-dependent mechanisms (Wu et al. 2017; Wu and Zhang 2017). TETs oxidize 5-methylcytosine (5mC) to 5-hydroxymethylcytosine (5hmC) that can then be actively reverted to cytosine through iterative oxidation and thymine DNA glycosylase (TDG)-mediated base excision repair (Ito et al. 2011; Kohli and Zhang 2013; Wu and Zhang 2017), which also occurs in neurons (Kaas et al. 2013; Li et al. 2014). Alike DNMTs, TET enzymes were identified to regulate synaptic function. TET1-dependent transcriptional control of activity-regulated genes was shown to be implicated in synaptic plasticity and memory extinction (Rudenko et al. 2013), whereas TET3 was described to modulate gene expression in response to global synaptic activity changes, thereby affecting homeostatic plasticity (Yu et al. 2015).

So far, studies were mainly focused on excitatory neurons. However, de-regulated expression of DNMTs was observed in patients with neuropsychiatric diseases like schizophrenia (Huang and Akbarian 2007; Sananbenesi and Fischer 2009; Matrisciano et al. 2013; Saradalekshmi et al. 2014; Benes 2015), associated to defects in the GABAergic system (Matrisciano et al. 2013). This strongly emphasizes a relevance of DNMTs for the function of inhibitory interneurons.

Redundant as well as discrete actions of DNMT1 and DNMT3a in the adult brain are reported in the literature. While in excitatory neurons DNMT1 and DNMT3a were described to have partially redundant functions (Feng et al. 2010), distinct roles of DNMT1 and DNMT3a were suggested by others (Morris et al. 2014; Morris et al. 2016). While DNMT3a seems to be crucial for learning (Morris et al. 2014), DNMT1 appears involved in anxiety (Morris et al. 2016), emphasizing the requirement for detailed inspection. We here started to approach the relevance of DNMT1-dependent DNA methylation in inhibitory cortical interneuron function by analyzing a conditional knockout (KO) mouse model, in which the gene encoding for DNMT1 was deleted in *Pvalb*-expressing interneurons, the most abundant subset of inhibitory neurons in the cerebral cortex (Druga 2009; Kelsom and Lu 2013; Lodato and Arlotta 2015; Bandler et al. 2017). *Dnmt1* deletion in these interneurons caused defects in interneuron activity, reminiscent of what was found for DNMT function in excitatory cortical neurons. Correlative transcriptome and methylome analysis of fluorescently activated cell sorting (FACS)-enriched parvalbumin (PV)-positive cortical interneurons of wild-type (WT) and *Dnmt1* KO mice indicated repressive DNMT1-dependent DNA methylation of genes related to endocytosis. Functional validation experiments confirmed that *Dnmt1* knockdown promotes clathrin-mediated endocytosis and recycling in cell-culture models. In turn, *Tet1* or *Tet3* depletion decreased the levels of clathrin-mediated endocytosis. This suggests an involvement of dynamic DNA methylation in the regulation of clathrin-dependent endocytosis, a process

crucial for the regulation of synaptic function (Kuromi and Kidokoro 2005). The physiological relevance of these findings for synaptic transmission was supported by electrophysiological recordings and HPLC measurements of extracellular GABA revealing a DNMT1-dependent modulation of synaptic vesicle replenishment and GABAergic transmission. Moreover, human brain sample analysis pointed to a potential implication of DNA methylation-dependent endocytosis regulation in the pathophysiology of temporal lobe epilepsy (TLE), a disease characterized by abnormal synaptic transmission.

Together, in addition to the most widely accepted connection of DNA methylation-dependent transcriptional control of synapse-associated genes in regulating synaptic function, DNMT1-dependent modulation of endocytosis could represent an additional mechanism for the orchestration of interneuron functionality.

Data and Materials Availability

RNA- and Methylated DNA Immunoprecipitation (MeDIP)-sequencing data of FAC-sorted *Pvalb-Cre/Dnmt1/tdTomato* samples will be provided on GEO. All other data are available in the main text or the supplementary materials.

Animals

The following mouse strains were used: C57BL/6 WT mice and transgenic mice on the C57BL/6 background including *Pvalb-Cre/tomato/Dnmt1* WT as well as *Pvalb-Cre/tomato/Dnmt1 loxP²* mice. The transgenic mice were established by crossing the *Pvalb-Cre* line (obtained from Christian Huebner, University Hospital Jena, Germany and described in Hippenmeyer et al. (2005)) with the *tdTomato* transgenic reporter mice (obtained from Christian Hübner, University Hospital Jena, Germany and described in Madisen et al. (2010)) and *Dnmt1 floxP²* mice, (B6;129Sv-Dnmt1^{tm4jae/J}), Jaenisch laboratory, Whitehead Institute; USA; Jackson-Grusby et al. (2001)). The *Dnmt1 floxP²* mice have LoxP-sites flanking exons 4 and 5 of the *Dnmt1* gene. Cre-mediated deletion leads to out-of-frame splicing from exon 3 to exon 6, resulting in a null *Dnmt1* allele (Jackson-Grusby et al. 2001). Transgenic mice are abbreviated as DNMT1 WT (wild-type) and DNMT1 KO (knockout) in the figures. The floxed *Dnmt1* allele was genotyped with forward 5'-GGCCAGTTGTGTGACTTGG and reverse 3'-CCTGGGCTGGATCTTGGGGA primer pairs resulting in a 334 bp WT and 368 bp mutant band. The *tdTomato* allele was genotyped using the set of following four primers: WT forward 5'-AAGGGAGCTGCAGTGGAGTA, WT reverse 3'-CCGAAAATCTGTGGGAAGTC, mutant forward 5'-CTGTTCTGTACGGCATGG, mutant reverse 3'-CTGTTCTGTACGGCATGG giving WT (297 bp) and mutant (196 bp) bands. The *PV-Cre* genotyping was performed by applying 5'-AAACGTTGATGCCGGTGAACGTGC forward and 3'-TAACATTCTCCACCGTCACTACG reverse primer resulting in a 214 bp fragment. All animal procedures were performed in strict compliance with the EU directives 86/609/EEG and 2007/526/EG guidelines for animal experiments and were approved by the local government (Thüringer Landesamt, Bad Langensalza, Germany and Landesamt für Natur, Umwelt und Verbraucherschutz Nordrhein-Westfalen, Recklinghausen, Germany). Animals were housed under 12 h light/dark conditions with ad libitum access to food and water.

Dissection of Adult Cortical Tissue

Mice were deeply anesthetized intraperitoneally with 50% chloral hydrate in phosphate buffered saline (PBS; pH 7.4, 2.5 µg chloral hydrate per g body weight). For immunohistochemistry, brains were perfused with PBS (pH 7.4) followed by 4% paraformaldehyde (PFA) in PBS (pH 7.4). Postfixation occurred overnight at 4 °C. Cryoprotection with 10% and 30% sucrose in PBS overnight was applied before freezing in liquid nitrogen and storage at -80 °C.

Tissue collection for HPLC and western blot analysis was also conducted with unfixed cortices, which were weighed before getting transferred into 1 mL of ice cold 1x DEPC-treated H₂O bidest and homogenized, using a tissue potter ("POTTER S" homogenizer, Braun Biotech International, Germany). Until usage, samples were stored at -80 °C.

Isolation and Primary Cultivation of Dissociated Embryonic Single Cells

As already described for adult dissections, pregnant dams were anesthetized by an intraperitoneal injection of 50% chloral hydrate. After death of the dam, all embryos were dissected out of both uterine horns and instantly decapitated. The brain was dissected in ice-cold and sterile filtered Gey's Balanced Salt Solution (GBSS; 1.53 mM CaCl₂, 3.66 mM KCl, 0.22 mM KH₂PO₄, 1.03 mM MgCl₂ × 6H₂O, 0.28 mM MgSO₄ × 7H₂O, 137.93 mM NaCl, 2.702 mM NaHCO₃, 0.84 mM Na₂HPO₄, and 5.56 mM D(+)-Glucose).

Dissociated embryonic medial ganglionic eminence (MGE)-derived single cells for primary culture were prepared from MGE explants dissected from coronal brain sections according to Zimmer et al. (2011). Briefly, embryonic brains were prepared in Krebs buffer (126 mM NaCl, 2.5 mM KCl, 1.2 mM NaH₂PO₄, 1.2 mM MgCl₂, 2.1 mM CaCl₂, 10 mM D(+)-Glucose, and 12.5 mM NaHCO₃), embedded in 4% low-melt agarose (Carl Roth, Germany) at 37 °C for coronal sectioning with a vibratome at 4 °C. MGE explants were collected in ice-cold Hanks balanced salt solution (HBSS, Invitrogen, USA) supplemented with 0.65% D(+)-Glucose. After incubation with 0.04% trypsin (Invitrogen) in HBSS for 17 min at 37 °C, cells were dissociated by trituration and filtering through nylon gauze (pore size 140 µm; Milipore). Dissociated neurons were plated on coverslips coated with 19 µg/mL laminin (Sigma-Aldrich, Germany) and 10 µg/mL poly-L-lysine (Sigma-Aldrich) at a density of 225 cells/mm² in Neurobasal Medium (Thermo Fisher Scientific, USA) supplemented with 1x B27 (Thermo Fisher Scientific), 100 U/mL penicillin, 100 µg/mL streptomycin, and 0.5 mM GlutaMax (Thermo Fisher Scientific). After incubation at 37 °C, 5% CO₂ in a humid atmosphere (95% H₂O) for 7 days in vitro (div), cells were fixed in 4% PFA in PBS (pH 7.4) for 10 min at room temperature.

Transfection with siRNA Oligos

For siRNA transfections of dissociated embryonic MGE cells of C57BL/6 WT mice, neuroblastoma (N2a) cells and cerebellar granular (CB) cells, reverse lipofection with Lipofectamin® 2000 or 3000 (Thermo Fisher Scientific) according to the manufacturer's protocol and as described in Zimmer et al. (2011) was applied using 15 nM control siRNA (BLOCK-iT Alexa Fluor red or green fluorescent oligo, Invitrogen) and *Dnmt1* siRNA, *Rab11* siRNA (Santa Cruz Biotechnology, USA) or 30 nM of *Tet1*, *Tet2*, or *Tet3* siRNA (Santa Cruz Biotechnology) for 5 h in Opti-MEM I Reduced Serum Medium without antibiotics (Thermo Fisher

Scientific). MGE-derived neurons were transfected after 6 div, whereas CB and N2a cells were plated on coverslips 1 day prior to transfection. Cells were cultured overnight at 37 °C, 95% H₂O and 5% CO₂ using the aforementioned cell line specific culture medium prior to fixation or transferred in a petri dish inserted in a 37 °C heated chamber filled with HBSS (Thermo Fischer Scientific) supplemented with 0.65% D(+)-Glucose, 10% FBS, 1% GlutaMAX (Thermo Fischer Scientific), 100 U/mL penicillin, 100 µg/mL streptomycin, and 25 µM of HEPES (Thermo Fisher Scientific) for live cell imaging.

Transferrin-Uptake Assay

Dissociated MGE cells of E15 C57BL/6 mice were grown on glass coverslips coated with laminin/poly-L-lysine for 1 div prior to transfection with siRNA oligos. Cells transfected with control and/or *Dnmt1*, *Tet1*, *Tet2*, and *Tet3* siRNA were incubated with transferrin-biotin 10 µg/mL biotinylated holotransferrin (Sigma-Aldrich) in prewarmed aforementioned culture medium and incubated for 2 h according to Akhtar and Hotchin (2001). Knockdown efficiency of the used siRNAs is depicted in Figure S3A. Cells were then fixed with 4% PFA in 1xPBS (pH 7.4) for 10 min. The cell surface-bound biotin molecules were quenched in 50 mM NH₄Cl in 1xPBS (pH 7.4) and permeabilized with TBS with 0.2% Saponin (Sigma-Aldrich). Cells were incubated for 1 h with a Rhodamine Red streptavidin conjugate (Jackson ImmunoResearch, USA) in TBS with 0.02% saponin for CB and MGE cells, and Alexa-488 streptavidin conjugate (Jackson ImmunoResearch, USA) for N2a cells. Cells were then washed in TBS with 0.02% saponin and stained with 4',6-Diamidin-2-phenylindol (DAPI) (100 ng/mL in 1xPBS (pH 7.4); Molecular Probes) for 5 min.

For inhibition of clathrin-dependent endocytosis, CB cells were incubated with 25 µM chlorpromazine (CPZ, Sigma-Aldrich; Marin et al. 2010; Vercauteren et al. 2010) in culture medium for 30 min at 37 °C prior to the transferrin uptake assay, which was also performed in the presence of 25 µM CPZ. After 2 h, cells were fixed in 4% PFA and treated as described previously.

To determine the impact of DNA-methylation on clathrin-dependent endocytosis, CB and N2a cells were treated with the specific inhibitor RG108 ([2-(1,3-dioxo-1,3-dihydro-2H-indol-2-yl)-3-(1H-indol-3-yl) propanoic acid]; 4 µM, Abcam, USA; Brueckner et al. 2005; Asgatay et al. 2014) or 0.04% DMSO in culture medium (as the inhibitor was dissolved in DMSO) for 24 h prior to the transferrin uptake assay, which was also performed in the presence of the inhibitor. After the 2 h, cells were fixed in 4% PFA and treated as described previously.

Quantitative Reverse Transcription PCR

RNA was isolated with Trizol[®] Reagent (Life Technologies, USA) according to manufacturer's guidelines and was used for cDNA synthesis using the SuperScript III or SuperScript IV First-Strand Synthesis Systems (Invitrogen). Quantitative PCR reactions for analyzing *Dnmt1*, *Tet1*, *Tet2*, *Tet3*, and *Hprt* quantities were performed using 10 ng cDNA of each sample and the innuMix qPCR DSGreen Standard Mastermix (Jena Analytik) on the qTOWER³ G thermocycler (Jena Analytik, Germany). Quantitative PCR reactions for analyzing *Wipf1*, *Zfyve9*, and *Rps29* quantities were performed using 10 ng cDNA of each sample and the iTaq Universal SYBR Green Supermix (BioRad, Germany) on the CFX96 thermocycler (BioRad, Germany). The following primer sequences (indicated as 5' → 3') were used: *Dnmt1* forw. GGT GAG CAT CGA

TGA GGA GA, rev. GCT GTG ACC CTG GCT AGA TA; *Tet1* forw. CAA CCA GGA AGA GGC GAC, rev. AGT CTG TAG ATT CGT CTT TCA CT; *Tet2* forw. GGT GCC TCC TTT TCT TTT GGT, rev. AGC AAT GAC AGT AGC CAG GT; *Tet3* forw. CAA GTG TGA GGT GCT GAA GA, rev. GTC TTG ACA GTC GCC CCT T; *Hprt* forw. GGC CAG ACT TTG TTG GAT TT, rev. CAG ATT CAA CTT GCG CTC AT; *Rab11* forw. GCA TAC TAT CGT GGA GCA GTA GG, rev. GGA ACT GCC CTG AGA TGA CG; *Wipf1* forw. AAC TAC CCA AGA TGC CTG TCC, rev. TTG TTC AAG GTG GGC TTC TC; *Zfyve9* forw. AAC CCA GGC CAT CAG TAT TCA, rev. CTG GAC CAT GAC TCC ATC TTC TA; *Rps29* forw. GAA GTT CGG CCA GGG TTC C, rev. GAA GCC TAT GTC CTT CGC GT; data were normalized to *Hprt* or *Rps29*. Results were analyzed via the $\Delta\Delta C_t$ -method.

Immunocytochemistry of Primary and Immortalized Single Cells

N2a and CB cells were washed with 1xPBS/0.2% Triton X-100 for 10 min prior to blocking with 5% normal goat serum in 1xPBS for 1 h. Primary antibodies were applied overnight at 4 °C, secondary antibody for 1 h at room temperature prior to DAPI staining (Molecular Probes) for 5 min.

The following primary antibodies were used: mouse anti-PV (Swant, Switzerland, 1:1000), rabbit anti-DNMT1 (Santa Cruz Biotechnology, 1:100), and mouse anti-RFP (Thermo Fisher Scientific, 1:500).

Following secondary antibodies were applied: goat Alexa 488 anti-mouse (Vector, UK, 1:1000), donkey Dylight 488 anti-rabbit (Jackson ImmunoResearch, USA, 1:1000), and goat Cy3 anti-mouse (Jackson ImmunoResearch, USA, 1:1000).

Electrophysiology

Slice preparation and electrophysiological recordings of the field potential were performed as described previously (Liebmann et al. 2009). Briefly, after decapitation of mice (8–10 weeks or 23 weeks of age), the brain was quickly removed, placed in ice-cold artificial cerebrospinal fluid (aCSF: 120 mM NaCl, 3.5 mM KCl, 1.3 mM MgSO₄ × 7 H₂O, 12.5 mM NaH₂PO₄ × H₂O, 2.5 mM CaCl₂ × 2 H₂O, 10 mM D(+)-Glucose, 25 mM NaHCO₃; and gassed with 5% CO₂, 95% O₂) and cut into coronal slices at a vibroslicer (VT 1000S, Leica Instruments). Slices (350 µm) were kept at room temperature in aCSF for at least 1 h until use.

For field-potential recordings, slices were transferred to an interface recording chamber. Slices were allowed to adapt to recording conditions for 1 h (oxygenated aCSF, 32 °C, flow 2–3 mL/min). Bipolar stimulating electrodes with a tip diameter of 100 µm (Science-Products, Germany) were placed onto layer VI of the motor cortex. Upon stimulation (pulse duration 50 µs), field potentials were recorded using glass microelectrodes (impedance 2–5 M Ω , filled with CSF) impaled into the cortical layer II/III of the motor cortex. Amplitudes of field excitatory postsynaptic potentials (fEPSPs) were analyzed. Data from field-potential recordings were collected with an extracellular amplifier (EXT-02, NPI, Germany), low-pass filtered at 4 kHz and digitally stored with a sample frequency of 10 kHz. Data acquisition and analysis were performed using the software Signal (Cambridge Electronic Design, UK). To determine the maximal amplitude of fEPSPs, the stimulus intensity was gradually increased (0–50 V, 5 V increment) for each experiment (interstimulus interval 30 s). The relationship between stimulus intensity and the evoked response was fitted by a sigmoid function: $R(i) = R_{\max}/(1 + \exp(i - ih))$, where $R(i)$ is the response at intensity

(i), R_{\max} is the maximal response and ih is the intensity at which half-maximal response was observed. After determination of the half-maximal stimulus intensity, paired-pulse stimuli were applied with interstimulus intervals of 15, 20, 30, 50, 80, 120, 180, 280, 430, 650, and 1000 ms.

Patch-clamp recordings of inhibitory postsynaptic currents (mIPSCs) in pyramidal neurons of motor cortex were performed in a submerged recording chamber mounted on an upright microscope (BX51WI, Olympus). Slices were continuously superfused with gassed aCSF (2–3 mL/min, 32 °C, pH 7.3). mIPSCs were recorded at a holding potential of -70 mV for at least 5 min in aCSF. Data analysis was performed off-line with the detection threshold levels set to 5 pA for mIPSCs. Recordings of mIPSCs were performed using a CsCl-based intracellular solution: 122 mM CsCl, 8 mM NaCl, 0.2 mM MgCl₂, 10 mM HEPES, 2 mM EGTA, 2 mM Mg-ATP, 0.5 mM Na-GTP, 10 mM QX-314 [N-(2,6-dimethylphenylcarbamoylmethyl)triethylammonium bromide], and pH adjusted to 7.3 with CsOH. dl-APV (30 μ M), CNQX (10 μ M), and tetrodotoxin (0.5 μ M) were added to the perfusate. The following parameters were determined: frequency and peak amplitude.

Vesicle depletion measurements were conducted as previously reported (Galarreta and Hestrin 1998). Whole-cell patch-clamp experiments for measurements of extracellular evoked IPSCs were performed on cortical pyramidal neurons of 13–18-week-old male or female *PV-Cre/tdTomato/Dnmt1 loxP²* mice and *PV-Cre/tdTomato/Dnmt1 WT*. Animals were anesthetized using isoflurane and afterward decapitated. Brains were gently removed and prepared for slicing in an ice-cold cutting solution containing 125 mM NaCl, 2.5 mM KCl, 1.25 mM NaH₂PO₄, 25 mM NaHCO₃, 25 mM D(+)-Glucose, 2 mM MgCl₂, and 1 mM CaCl₂. During all experiments, slices were continuously perfused with carbogen (95% O₂ and 5% CO₂). The frontal part of the brain was removed and coronal slices of 300 μ m of the visual cortex were cut with a Leica vibratome at an angle of 15°. Before an experiment was started, slices had to rest for 30 min at 35 °C. Afterward slices were stored at room temperature. Recordings were performed at a temperature of 30–34 °C while slices were perfused with oxygenated aCSF (125 mM NaCl, 2.5 mM KCl, 1.25 mM NaH₂PO₄, 25 mM NaHCO₃, 25 mM D(+)-Glucose, 1 mM MgCl₂, and 2 mM CaCl₂). Recordings were obtained with an amplifier (ELC-03-XS, npi electronics, Germany). Data were low-pass filtered at 10 kHz and digitized at a sampling rate of 20 kHz using a data acquisition board (PCIe 6143, National Instruments) on a Windows-based Computer (Dell). Recordings were made with the custom written program Wavesurfer (version 0.961, Janelia, Howard Hughes Medical Institute). Extracellular stimulation was generated with an isolated stimulator (Digitimer Ltd model DS2A) connected to a large tip patch-clamp electrode. Borosilicate glass pipettes (diameter outside 1.05, inside 1.50, and length 100 mm) with a resistance of 6–9 M Ω were filled with 135 mM K-gluconate, 4 mM KCl, 10 mM HEPES, 4 mM MgATP, and 0.3 mM GTP. Glass pipettes were used to perform whole-cell somatic current recordings from layer II/III pyramidal neurons. Pyramidal neurons were identified according to their pattern of firing in response to depolarizing current steps (500 ms duration). Inhibitory synaptic currents were recorded at a holding potential of 0 mV in the presence of the AMPA/kainate receptor antagonist DNQX (10 μ M) and NMDA receptor antagonist APV (30 μ M) to block EPSCs. IPSC current amplitudes were determined in Matlab with custom-written software. Vesicle pool size was calculated as described before (Schneeggenburger et al. 1999). Data are

presented as mean \pm SEM if not indicated otherwise. For statistical analysis, a nonparametric Wilcoxon–Mann–Whitney test was performed.

Isolation and Dissociation of Adult Cortical Neurons for FACS

The optimized protocol used to collect the material for DNA- and RNA-sequencing was modified based on different protocols (Brewer 1997; Eide and McMurray 2005; Brewer and Torricelli 2007; Saxena et al. 2012). Adult brains were dissected in GBSS (1.53 mM CaCl₂, 3.66 mM KCl, 0.22 mM KH₂PO₄, 1.03 mM MgCl₂ \times 6H₂O, 0.28 mM MgSO₄ \times 7H₂O, 137.93 mM NaCl, 2.7 mM NaHCO₃, 0.84 mM Na₂HPO₄, 5.56 mM D(+)-Glucose, pH 7.4) supplemented with 0.65% D(+)-Glucose. Cortical hemispheres were dissected and subsequently handled separately. All following volumes are calculated per cortical hemisphere, which were cut into small pieces and transferred to 5 mL HBSS w/o Ca²⁺ and Mg²⁺ supplemented with 7 mM HEPES, 100 U/mL penicillin, 100 μ g/mL streptomycin, and 0.65% D(+)-Glucose and washed twice. The tissue was then transferred to 5 mL prewarmed (20 min at 37 °C) trypsin/EDTA (Life technologies) supplemented with 132 mM trehalose (Sigma-Aldrich), 100 U/mL penicillin, 100 μ g/mL streptomycin, 10 mM HEPES, and 600 U DNase (Appllichem, Germany) and incubated for 30 min at 37 °C, rotating the samples every 5 min. Samples were washed with 2.1 mL prewarmed DMEM/F12 supplemented with 10% FBS, 100 U/mL penicillin, 100 μ g/mL streptomycin, and 132 mM trehalose. After adding 0.9 mL prewarmed HBSS containing 10 mg/mL collagenase type 2 (Worthington, Great Britain) samples were incubated for 25 min at 37 °C rotating every 5 min and then washed with 2 mL prewarmed DMEM/F12 supplemented with 10% FBS, 100 U/mL penicillin, 100 μ g/mL streptomycin, 3.3 mM EDTA, and 132 mM trehalose prior to cool down on ice for 2 min. Dissolving of samples occurred in 1.5 mL DMEM/F12 supplemented with 10% FBS, 100 U/mL penicillin, 100 μ g/mL streptomycin, and 132 mM trehalose. Trituration was performed using fire-polished and heat-treated (180 °C for 8 h) glass capillaries of three different diameters (about 500; 250; and 100 μ m), which were coated with DMEM/F12 supplemented with 10% FBS, 100 U/mL penicillin, and 100 μ g/mL streptomycin prior to use. Mechanical dissociation was performed by pipetting up and down gently 3–5 times for each diameter starting with the largest diameter, avoiding air bubbles. After each step, the supernatant was collected in 1 mL DMEM/F12 supplemented with 10% FBS, 100 U/mL penicillin, 100 μ g/mL streptomycin, and 132 mM trehalose was added to the original sample. After trituration with the smallest glass capillary, suspension was filtered through nylon gauze (80–100 μ m) and centrifuged for 5 min at 160 \times g, 4 °C. After supernatant removal, the pellet was dissolved in 4 mL HBSS w/o Ca²⁺ and Mg²⁺ supplemented with 7 mM HEPES, 100 U/mL penicillin, 100 μ g/mL streptomycin, 0.65% D(+)-Glucose, and 132 mM trehalose. After centrifugation (5 min, 160 \times g, 4 °C), the pellet was dissolved in 1 \times PBS (pH 7.4) with 30% Percoll (Sigma-Aldrich) and 132 mM trehalose to perform a density gradient centrifugation for 10 min at 500 \times g and 4 °C. The supernatant was removed and the pellet was dissolved in 250 μ L HBSS w/o Ca²⁺ and Mg²⁺ supplemented with 7 mM HEPES, 100 U/mL penicillin, 100 μ g/mL streptomycin, 0.65% D(+)-Glucose, and 132 mM trehalose for FACS. The nonoptimized protocol was performed accordingly without trehalose in the buffers and skipping the collagenase treatment as well as percoll density centrifugation step.

FACS Enrichment of tdTomato Cells

Cell suspensions subjected to FACS were prepared from the cortical hemispheres of adult 6-months old *PV-Cre/tdTomato/Dnmt1* WT as well as *PV-Cre/tdTomato/Dnmt1 loxP²* mice. Following the addition of DAPI, cells were sorted using an ARIA III FACS sorter (BD Biosciences, USA) with the maximal flow rate of six. The tdTomato reporter was excited by a 561 nm yellow/green solid-state laser and emission signal was detected in a range of 579–593 nm. According to their forward scatter/side scatter (FSC/SSC) criteria followed by cell doublet exclusion via a FSC-H versus FSC-W criterium, DAPI-negative living cells were sorted based on a distinctive tdTomato signal. Cells of interest were collected in HBSS w/o Ca²⁺ and Mg²⁺ supplemented with 7 mM HEPES, 100 U/mL penicillin, 100 µg/mL streptomycin, 0.65% D(+)-Glucose, and 132 mM trehalose at 4 °C and pelleted by centrifugation (10 min at 10 000 × *g*, 4 °C). Enriched tdTomato cells of one hemisphere were prepared for RNA-sequencing, while cells of the contralateral hemisphere were subjected to DNA-isolation for MeDIP-sequencing for each brain used. For RNA isolation, pellets were dissolved in 500 µL Trizol[®] Reagent (Life Technologies) and subsequently frozen on dry ice. For MeDIP-Seq analysis, cell pellets were frozen at –80 °C until further use. Only male mice were used for RNA and MeDIP sequencing.

RNA/DNA Isolation of Adult Tissue and FAC-Sorted Cells

Adult cortical hemispheres were dissected from whole brain and frozen in liquid nitrogen as described above. For RNA-sequencing, the tissue was subjected to standard RNA isolation procedure using Trizol[®] Reagent (Life Technologies). The FACS-enriched tdTomato cells were processed accordingly, with additional application of GlycoBlue (Thermo Fisher Scientific) to a final concentration of 0.2% during RNA precipitation for better visualization of the pellet.

DNA isolation of FACS-enriched tdTomato cells was performed using QIAamp DNA Micro Kit (Quiagen, Germany) according to manufacturer's instruction and checked for integrity by capillary gel electrophoresis (Bioanalyzer, Agilent Technologies, Inc., USA).

RNA and MeDip Sequencing of FACS-Enriched tdTomato Cells

RNA was isolated following the Trizol[®] Reagent protocol according to manufacturer's instructions. RNA quality was assessed by measuring the RIN (RNA Integrity Number) using the fragment analyzer from Advanced Analytical (USA). Library preparation for RNA-Seq was performed applying the TruSeq RNA Sample Prep Kit v2 (Illumina, Cat. N°RS-122-2002, USA) starting from 50 ng of total RNA. Accurate quantitation of cDNA libraries was performed by using the QuantiFluor dsDNA System (Promega, USA). The size range of final cDNA libraries was determined applying the DNA chip on the fragment analyzer (average 350 bp; Advanced Analytical). cDNA libraries were amplified and sequenced by using the cBot and HiSeq2000 from Illumina (SR; 1 × 50 bp; ~30–40 million reads per sample). Sequence images were transformed with Illumina software BaseCaller to bcl files, which were demultiplexed to fastq files with CASAVA v1.8.2. Quality check was done via fastqc (v. 0.10.0, Babraham Bioinformatics, UK). Read alignment was performed using STAR (v2.3.0; Dobin et al. 2013) to the mm10 reference genome. Data

were converted and sorted by samtools 0.1.19 and reads per gene were counted via htseq version 0.5.4.p3. Sequencing data will be deposited in NCBI's Gene Expression Omnibus, and are accessible through GEO Series upon acceptance of the manuscript.

For genome-wide methylation analysis, we applied immunoprecipitation methods for the enrichment of 5-methylcytosines. Specifically, 100 ng of genomic DNA were used as starting material. The methylated-DNA IP kit from zymo research (Zymo Research Corp., D5101, USA) was applied according to manufacturer's instructions. The product of the IP and control reaction was then used for preparation of Illumina compatible libraries according to the TruSeq Nano DNA Library Prep Kit (Cat. N° FC-121-4001). Libraries were sequenced on a HiSeq 2000 yielding 50 bp single end reads. The sequencing reads were demultiplexed using the Illumina CASAVA tool and sequence quality was checked using FASTQC (<http://www.bioinformatics.babraham.ac.uk/projects/fastqc/>). The reads were then aligned to the genome of *Mus musculus* (mm10) using Bowtie 2 (versions 2.0.2) with standard parameters. Differentially methylated regions were identified using the MEDIPS package for R (version 1.16.0; Lienhard et al. 2014) with a window size of 700 bp and a minimum coverage of 5% of the window length. A detailed description of the analysis pipeline can be found in Halder et al. (2016).

Analysis of Mouse Sequencing Data

Normalization of raw counts and differential gene expression analysis were performed using the DESeq2 R package (v 1.12.3; Love et al. 2014). Genes were considered differentially expressed with a Benjamini-Hochberg adjusted *P* value *P* < 0.05.

For the gene list overlaps between differentially expressed and methylated genes, it was considered that several differentially methylated sites may be annotated to one gene and were quantified using the Jaccard coefficient. Absolute numbers of differentially methylated genes were determined without regard to multiple sites of differential methylation. Significance of enrichment of methylated genes was calculated using Fisher's Exact test.

Gene lists were submitted to the Database for Annotation, Visualization and Integrated Discovery (DAVID, <https://david.ncifcrf.gov>) for gene ontology (GO) or KEGG pathway term enrichment analysis. Results of GO enrichment analysis were visualized in a bar diagram including the respective Benjamini-Hochberg corrected *P* value, the number of genes, and the enrichment fold change included in a certain term. Heat maps were generated using R package pheatmap (<https://CRAN.R-project.org/package=pheatmap>). For heat maps showing comparison between two datasets, data were normalized to WT and log₂ fold-change to KO is depicted. KEGG pathway was visualized using R package pathview (Luo and Brouwer 2013).

Human TLE Patients

Biopsies of human hippocampal tissue of 115 patients with chronic pharmaco-resistant TLE, who underwent surgical treatment in the Epilepsy Surgery Program at the University of Bonn Medical Center were selected for gene expression and DNA methylation analysis. In all patients, presurgical evaluation using a combination of noninvasive and invasive procedures revealed that seizures originated in the mesial

temporal lobe (Kral et al. 2002). All procedures were conducted in accordance with the Declaration of Helsinki and approved by the Ethics Committee of the University of Bonn Medical Center. Informed written consent was obtained from all patients. Clinical characteristics of the TLE patients are described in Table S4.

Human mRNA Expression and DNA Methylation analysis

Sample preparation and data analysis of the human hippocampi were performed as described previously (Johnson et al. 2015; van Loo et al. 2015; Schulz et al. 2017). Expression data for the selected endocytosis genes were analyzed by Illumina's GenomeStudio Gene Expression Module and normalized using Illumina BeadStudio software suite by quantile normalization with background subtraction. DNA methylation data were prepared using bisulfite converted genomic DNA (Zymo EZ DNA Methylation kit #D5001; Zymo Research Corp.) on the Illumina (San Diego, CA, USA). Data analysis was done using GenomeStudio version 2011.1 and the HumanMethylation450 manifest version 1 (Illumina, Schulz et al. 2017). For genes annotated in endocytosis-related terms, the correlation and significance were calculated, followed by the fold-change expression between low (1 seizure/month) and high seizures (150 seizures/month) for all significant correlated genes.

Methylation profiles for *Wipf1* were mapped to human (hg19) and mouse (mm10) reference genome on UCSC genome browser, and orthologue mapping was extracted from ensemble database.

Microscopy and Image Data Analysis

Immunohistochemistry staining of adult tissue sections or immunocytochemistry of stained cell culture was taken either with an inverted confocal laser scanning microscope TCS SP5 (Leica Microsystems, Germany) or with an inverted transmitted-light microscope Axio Cellobserver Z1 equipped with MosaicX module for tile scanning and Apotome for confocal like imaging (Carl Zeiss Microscopy, Germany). Photographs were analyzed using the free Fiji software (Schindelin et al. 2012).

Analysis of cell number in adult sections and in cell culture was performed with Fiji cell counter plugin. Counted cell numbers in section analysis were normalized to the area of the counted region. For cell-culture experiments, the ratio to DAPI positive cells per picture was calculated. In case of double labeling, the percentage of colocalization was measured.

For fluorescence intensity measurement, each experimental design was imaged at one particular microscope with same settings regarding exposure time and light intensity at the Cellobserver Z1 or laser power, gain, and spectral settings at the SP5 LSM. Fluorescence intensity measurement of the processes of the cells was applied for the transferrin assay. For each picture, background correction was performed subtracting the mean fluorescent intensity from three background areas. Mean fluorescent intensity of the *Dnmt1* siRNA treated cells was normalized to control siRNA. Photoshop CC was applied for image illustration. Boxplots were plotted using R. Significance was analyzed with two-tailed Student's *t*-test or two-way ANOVA. Significance levels: *P* value < 0.05*; *P* value < 0.01**; and *P* value < 0.001***.

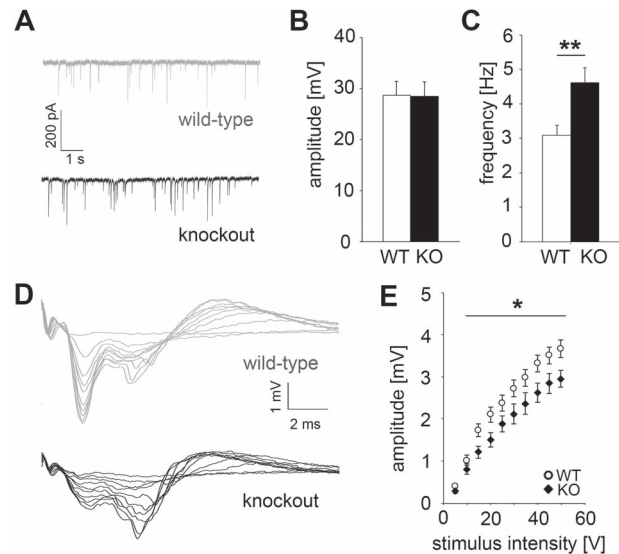


Figure 1. *Dnmt1* deficiency in *Pvalb*-expressing interneurons causes alterations in cortical inhibition. (A–C) Intracellular patch-clamp recordings (mIPSCs) of deep layer pyramidal cells of *Pvalb-Cre/tdTomato/Dnmt1 loxP2* (KO) and WT mice (two-way ANOVA, ***P* < 0.01; *n* = 8 cells of *N* = 3 brains per genotype). (D, E) Extracellular field recordings in the motor cortex of acute brain slices from 12-week-old *Pvalb-Cre/tdTomato/Dnmt1 loxP2* (KO) and WT mice (two-way ANOVA, **P* < 0.05; *n* = 9 slices for WT and *n* = 12 slices for KO; *N* = 3 different brains per genotype).

Results

Cortical Inhibition is Affected by *Dnmt1* Deletion

Inhibitory GABA-positive forebrain interneurons are elementary key players in cortical information processing, plasticity as well as learning and memory formation (Hensch and Fagioli 2005; Letzkus et al. 2015). Albeit they prominently express DNMT1 at adult stages (Kadriu et al. 2012), nothing is known about the implications of DNMT1 in regulating synaptic function in these neurons. As disturbed GABAergic transmission, often associated with defective DNMT expression and function, is implicated in a wide range of neuropsychiatric diseases like schizophrenia or epilepsy (Marin 2012), we here approached the role of DNMT1-dependent DNA methylation in the regulation of synaptic function in adult inhibitory cortical interneurons. For this, we established a conditional KO mouse model, in which the gene encoding for DNMT1 was deleted in *Pvalb*-expressing interneurons (Fig. S1A–G; *Pvalb-Cre/tdTomato/Dnmt1 loxP2* mice with *Pvalb-Cre/tdTomato* mice used as WT controls), the most abundant subset of inhibitory neurons in the forebrain (Kelsom and Lu 2013; Lodato and Arlotta 2015). *Pvalb* expression starts from the fifth week of life (Madisen et al. 2010). Hence, interneuron development, shown to depend on DNMT1 function (Pensold et al. 2017), is not affected by *Dnmt1* deletion in these mice.

Reminiscent of Meadows et al. (2015) reporting increased frequencies of mEPSCs upon DNMT inhibition, we found augmented frequencies of mIPSCs in excitatory principal cortical neurons in *Pvalb-Cre/tdTomato/Dnmt1 loxP2* brain slices, pointing to changes in presynaptic function of inhibitory interneurons (Figure 1A–C). Consistently, we detected elevated extracellular GABA concentrations measured by HPLC in the cortices of *Dnmt1*-deficient mice, while the overall interneuron number was unchanged (Fig. S1H–I). This points to increased GABA

release, which fits to the reduced amplitudes of field potentials measured at higher stimulus intensities (Fig. 1D,E). Hence, corresponding to what was described for excitatory neurons (Levenson et al. 2006; Nelson et al. 2008; Sweatt 2016), our data indicate a role of DNMT1 in the modulation of synaptic transmission in inhibitory cortical interneurons.

Correlative Transcriptome and Methylome Analysis of FAC-Sorted Cortical Interneurons Propose Endocytosis-Related Genes as DNMT1 Targets

DNMT1 regulates gene expression predominantly through its DNA-methylating activity often correlated with transcriptional repression (Bestor 2000; Robertson 2002). To investigate in detail how DNMT1 acts on GABAergic transmission, we aimed to identify target genes by correlative global methylome and transcriptome analysis of *Dnmt1*-deficient and WT interneurons that were enriched by fluorescence-activated cell sorting (validation of the procedure is depicted in Fig. S2A–H).

RNA-sequencing revealed 3868 differentially expressed genes (DEG) in *Pvalb-Cre/tdTomato/Dnmt1* KO interneurons, of which a significant number (645 genes; 16.7% of all DEG) showed simultaneously differential methylation (DMG; Fig. 2A–D; Table S1; $P = 2.2E - 16$, Fisher's Exact test for gene set enrichment analysis; enrichment fold-change $F_c = 0.434$). Consistent with the known function of DNMT1 performing repressive DNA methylation, decreased average methylation levels for genes that are upregulated in expression were identified in consequence of *Dnmt1* deletion (Fig. 2C). For the majority of the genes altered in expression and DNA methylation (72.2%), we determined an inverse correlation of changes in DNA methylation and expression level (upper left and lower right quadrant in Fig. 2E). Of note, differential methylation mostly affects gene bodies (Fig. 2C,F, exons and introns). Genes found increased in expression and reduced in DNA methylation levels (lower right quadrant in Fig. 2E) represent potential targets of repressive DNA methylation-dependent gene regulation by DNMT1 in WT. Functionally, as revealed by GO-enrichment and KEGG-pathway analysis, many of these genes were associated to membrane, endocytosis, and endosomes (Figs 2G,H and S2I, Table S2), with the highest enrichment fold-changes obtained for the GO terms endocytosis and early endosome membrane (Fig. 2G). In particular, genes relevant for clathrin-dependent endocytosis like *Cltc* and *Dnm3* were increased in expression and reduced in methylation in *Dnmt1*-deficient interneurons (Figs 2H and S2I, Table S2). A potential function of DNMT1 in regulating endocytosis is reinforced by GO analysis of all significantly up-regulated genes upon *Dnmt1* deletion irrespective of changes in their methylation level (Fig. 2I).

In contrast to endocytosis-related genes, most of synaptic activity and transmission-associated genes collected in GO categories like synapse, postsynaptic membrane, or chemical synaptic transmission were down-regulated upon *Dnmt1* deletion (Fig. 3A). Similarly, most genes of the GO terms voltage-gated ion channels, solute carriers, and glutamate receptors, relevant for synaptic transmission, were also decreased in expression in the KO samples (Fig. 3B,C). Transcriptional down-regulation points to indirect or secondary effects of *Dnmt1*-deletion. We already reported that a crosstalk of DNMT1 with histone modifying complexes regulates crucial aspects of cortical interneuron development (Symmank et al. 2018). DNMT1 modulates histone modifications by regulating the

transcription of genes encoding for the enzyme complexes as well as by interacting with histone modifying enzymes at protein level in neuronal and non-neuronal cells (reviewed in Symmank and Zimmer 2017)). Such noncanonical actions of DNMT1 could also play a role in adult interneurons. In support of this, histone modification-associated genes are changed in transcription in *Dnmt1*-deficient interneurons (Table S3). Some of the solute carrier, glutamate receptor and voltage-gated ion channel-related genes revealed to be changed in expression also show altered methylation levels after *Dnmt1* deletion. However, many of them even displayed increased methylation levels (Fig. 3B, blue dots in upper left quadrant). This could be explained by potential compensatory actions of DNMT3a. As we did not detect significantly altered *Dnmt3a* levels in *Dnmt1*-deficient interneurons (Fig. S2J), these might occur independently of its transcriptional regulation. In contrast to *Dnmt3a*, various other genes related to DNA methylation and demethylation processes are changed in expression in *Dnmt1*-deficient cells (Table S3), which can elicit diverse changes in methylation profiles. However, within the scope of this study, we aimed to analyze putative targets of repressive DNA methylation executed by DNMT1. Hence, for further analysis, we focused on genes that were increased in expression and reduced in methylation for further analysis, among which endocytosis-related genes were significantly enriched. As defective endocytosis induced by loss of *Dnm1* (encoding for Dynamin 1) was reported to affect inhibition by impairing synaptic vesicle recycling (Ferguson et al. 2007), we next validated DNMT1-dependent endocytosis regulation.

DNMT1 Regulates Clathrin-Mediated Endocytosis and Endosomal Recycling

To functionally validate a DNMT1-dependent modulation of clathrin-mediated endocytosis, we performed the transferrin uptake assay in dissociated primary cells from the embryonic MGE. Embryonic MGE-derived cells, known to represent the major source of PV-positive cortical interneurons (Kelsom and Lu 2013), express *Dnmt1* (Pensold et al. 2017) and display a maturing GABAergic identity with prominent neurite outgrowth and distinguished axons after 7 div (Fig. S3B–G).

Consistent with the decreased methylation and increased expression of endocytosis-related genes in *Dnmt1*-deficient cortical interneurons (Fig. 2G,H), in vitro depletion of *Dnmt1* by siRNA oligos elicited an elevation of clathrin-dependent uptake of biotinylated transferrin in MGE-derived embryonic interneurons (Fig. 4A–C). Similar results were obtained when we depleted *Dnmt1* in immortalized CB and neuroblastoma (N2a) cells (Fig. S4A–C), as well as upon treatment with the selective inhibitor RG108 that interacts with the active site of DNMT1, and thereby inhibits DNA methylation (Fig. S4F–H; Brueckner et al. 2005; Asgatay et al. 2014). In turn, blocking clathrin-dependent endocytosis with the specific inhibitor CPZ (Marin et al. 2010; Vercauteren et al. 2010) reversed the *Dnmt1* siRNA-induced elevation of transferrin uptake (Fig. S4I–K).

Depletion of Tet1 and Tet3 Caused Reduced Levels of Clathrin-Mediated Endocytosis

DNA methylation patterns are highly dynamic in differentiating as well as adult neurons shaping the genomic landscape during brain development and adult function (Lister et al. 2013). Indeed, methylated cytosines can be actively reverted to unmethylated

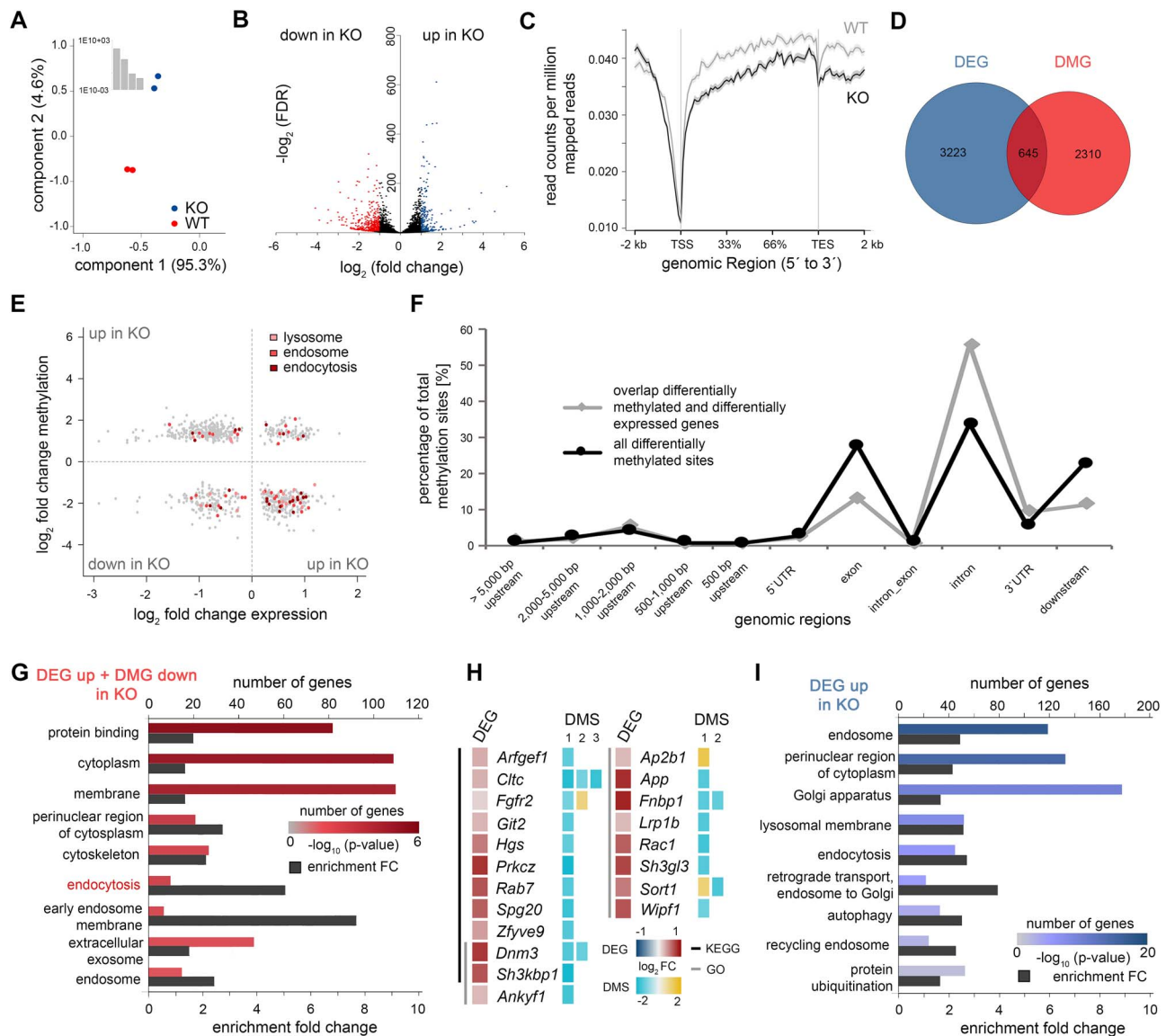


Figure 2. *Dnmt1* deficiency in *Pvalb*-expressing interneurons causes changes in the expression and DNA methylation of endocytosis-related genes. (A) PCA plot of FAC-sorted *Pvalb*-Cre/*tdTomato Dnmt1* WT and *Pvalb*-Cre/*tdTomato Dnmt1* KO samples analyzed by RNA sequencing. Pooled samples from $N=6$ mice per genotype (6 months) were analyzed in technical duplicates. (B) Volcano plot of transcriptional changes between WT and KO cortical interneurons determined by RNA-sequencing (Benjamini-adjusted $P < 0.05$; fold change > 2 for colored labeled genes). (C) Methylation plot of the average methylation levels of upregulated genes (DEG) in adult KO (dark gray) compared with WT interneurons (light gray; TSS = transcription start site, TES = transcription end site). (D) Venn diagram of differentially expressed (DEG) and methylated genes (DMG; $P = 2.2E-16$; Fisher's Exact test). (E) Scatter plot of genes with simultaneously altered expression and DNA methylation ($P < 0.05$; Benjamini adjusted) upon *Dnmt1* deletion. (F) Plotting the frequency of differentially methylated sites comparing 6-months-old *Dnmt1* KO and WT interneurons against genomic regions (black graph: considering all genes showing differential methylation; gray graph: considering all genes that were simultaneously differentially expressed and methylated between KO and WT interneurons). Exon_Intron refers to sites spanning the splice site. (G) Bar plot of GO and KEGG pathway (red labeled term) analysis of all genes found increased in expression and decreased in DNA methylation in KO ($P < 0.05$; Benjamini adjusted). (H) Heat-map of DEG and DMG extracted from the KEGG pathway and GO term endocytosis (for KEGG pathway see also Fig. S21). Depicted are the changes in the KO samples normalized to WT values for DEG and individual differentially methylated sites (DMS). (I) Bar plot of GO terms found significantly enriched for the genes that were upregulated upon *Dnmt1* deletion in adult *Pvalb*-Cre-expressing cortical interneurons.

cytosines through TET-mediated mechanisms (Guo et al. 2011a; Wu and Zhang 2017). Hence, we next wondered whether endocytic rates can likewise be modulated by TET-dependent actions. For this, we depleted *Tet1*, *Tet2*, and *Tet3* expression in MGE cells using sequence-specific siRNA oligos and performed the transferrin uptake assay, resulting in a significant reduction of endocytosed transferrin upon *Tet1* and *Tet3* depletion (Fig. 4D–H).

Consistently, we revealed for *Wipf1* and *Zfyve9*, two endocytosis-related genes found up-regulated in expression and reduced in methylation in *Dnmt1*-deficient interneurons (Fig. 2H), contrary expression changes in response to *Dnmt1* and *Tet1* siRNA in CB cells (Fig. 4I), which we used as a model system due to the unavailability of *Tet* KO mice. While *Dnmt1* siRNA elicited a significant increase in expression levels, *Tet1* siRNA had the

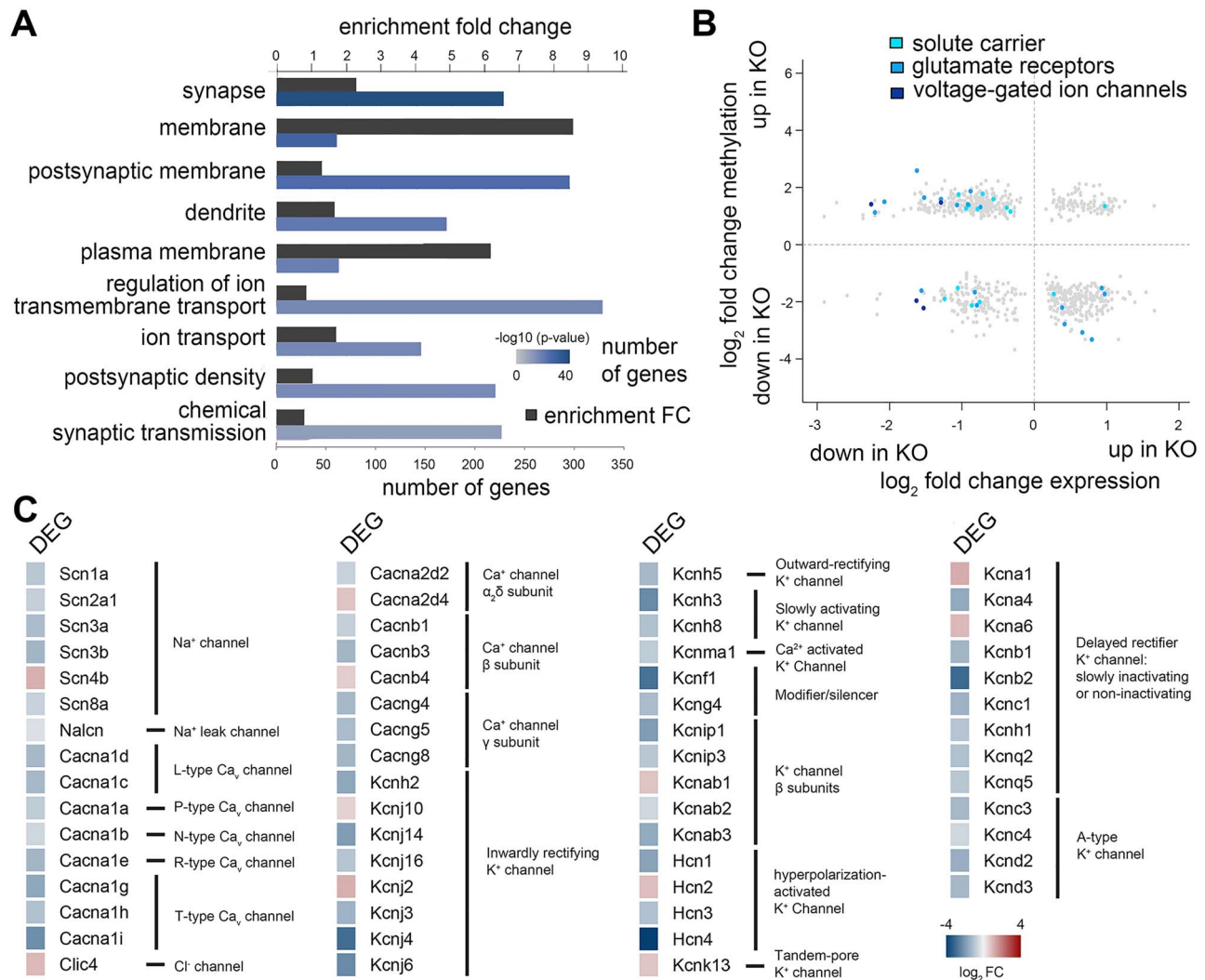


Figure 3. Synapse-related genes are downregulated by *Dnmt1* deletion in PV interneurons, and only few are changed in their DNA methylation level. (A) GO terms found significantly enriched for the genes that were down-regulated upon *Dnmt1* deletion in adult *Pvalb-Cre*-expressing cortical interneurons. (B) Scatter plot illustrating the differential methylation and gene expression between adult FACS-enriched *PV-Cre/tdTomato/Dnmt1 loxP²* (KO) and WT cells with positive ratios representing an upregulation of gene expression and increased methylation levels in KO samples. Solute carrier, glutamate receptors, and voltage-gated ion channels-related genes as determined by GO analysis are highlighted by the different graded bluish colored dots. (C) Heat-map illustrating transcriptional changes of significantly expressed genes between WT and KO interneurons collected in the GO-term voltage gated ion channels. Changes in expression in KO samples were normalized to WT levels ($P < 0.05$, Benjamini adjusted). Number $n = 6$ hemispheres of six different mice per genotype for RNA-Seq and MeDIP-Seq. WT: wild-type; KO: knockout.

opposite effect on the expression of both genes (Fig. 4I). This is in line with reduced levels of endocytosed transferrin upon *Tet1* siRNA treatment, which we determined for these cells (Fig. S4D–E). In sum, this points to a responsiveness of clathrin-mediated endocytosis towards TET-dependent actions and proposes an implication of dynamic DNA methylation in the fine-tuning of clathrin-mediated endocytosis through the regulation of associated genes.

DNMT1 Affects the Replenishment of Synaptic Vesicles

Endocytosis at synapses is implicated in synaptic vesicle replenishment, thereby influencing synaptic transmission (Kuromi and Kidokoro 2005). Hence, DNMT1 could influence GABAergic transmission by acting on endocytosis-mediated recycling of synaptic vesicles. In support of this, we found that the elevated

levels of endocytosis induced by *Dnmt1* depletion are accompanied by augmented recycling back to the membrane and subsequent exocytosis (Fig. S4L–O), as shown by the pulse-chase assay commonly used to investigate endocytic-based recycling of transferrin (Xie et al. 2016). Together, this suggests an important role of DNA methylation in endocytosis regulation and downstream processes across different neuronal cell types.

To validate whether DNMT1 indeed affects synaptic vesicle replenishment, patch-clamp recordings were performed in pyramidal neurons of layer II/III in slices from *Pvalb-Cre/tdTomato/Dnmt1 loxP²* and WT mice to measure the recovery of IPSCs after vesicle depletion induced by repeated extracellular stimulations (Fig. 4J–L). While the comparison of the vesicle pool size at 10 Hz revealed no significant difference between KO (13 ± 1.95) and WT mice (18.41 ± 2.93 ; normalized units), the recovery of IPSCs was improved in the

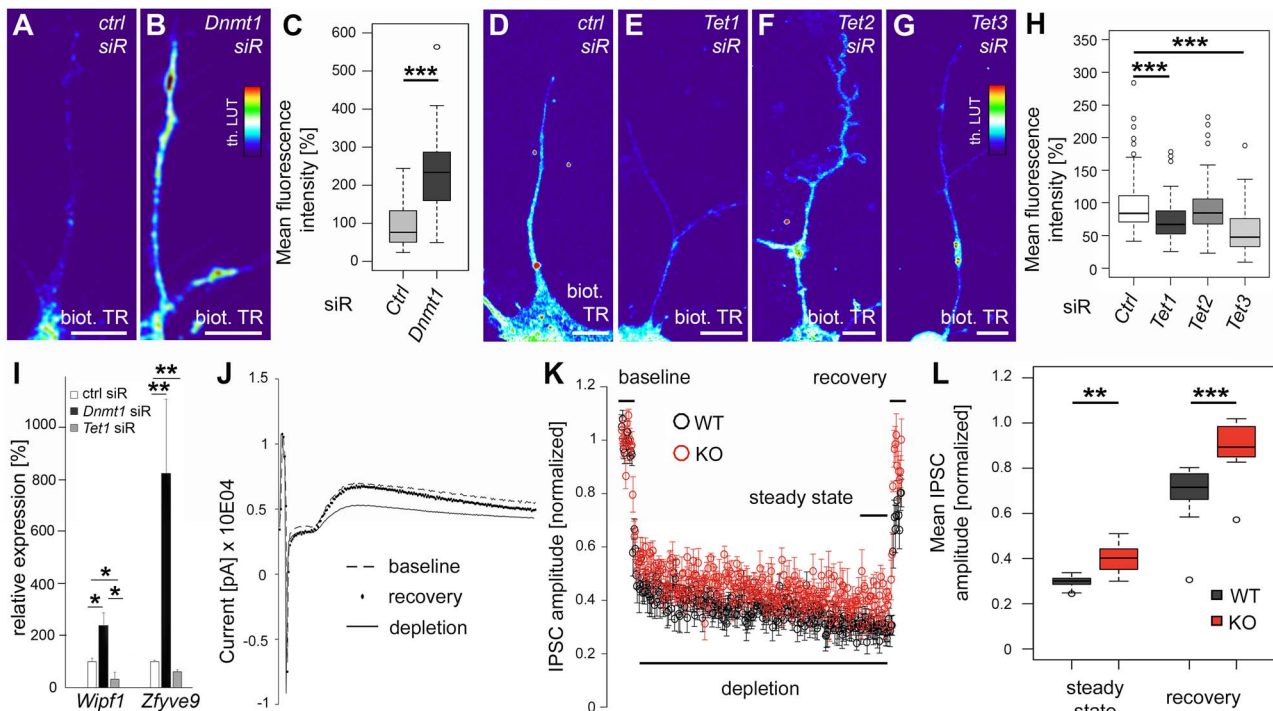


Figure 4. DNMT1, TET1, and TET3 regulate clathrin-dependent endocytosis in vitro and Dnmt1 deletion affects synaptic vesicle recycling. (A–C) Transferrin-uptake assay with dissociated MGE cells (E15 + 7 div) transfected with control (A, $n = 20$) or *Dnmt1* siRNA (B, $n = 19$ cells). Fluorescence intensities are illustrated as color-coded heat-maps (thermal LUT) and quantified in C. (D–H) Transferrin-uptake in MGE-derived cells treated with control (D, $n = 100$), *Tet1* (E, $n = 70$ cells), *Tet2* (F, $n = 70$ cells) or *Tet3* siRNA (G, $n = 73$ cells) illustrated as thermal LUT and quantified in H. Student's *t*-test, *** $P < 0.001$. (I) *Dnmt1* and *Tet1* depletion in CB cells had contrary effects on the expression levels of the endocytosis-related genes *Wipf1* and *Zfyve9* as measured by qPCR normalized against *Rps29*; $N = 3$. (J) Example of averaged traces measured for extracellular evoked IPSCs from layer II/III pyramidal neurons in brain slices of *Dnmt1*-deficient mice. Averaged baseline and recovery IPSCs of 10 responses obtained at a frequency of 0.2 Hz and vesicular depletion responses during a 10 Hz stimulus train (averaged trace of 270 responses). (K) Comparison of synaptic depletion. Each circle represents the average of all IPSC amplitudes from *Pvalb-Cre/tdTomato/Dnmt1 loxP2* (KO) ($n = 4$; red symbols) or *Pvalb-Cre/tdTomato* WT mice ($n = 7$). (L) Mean IPSC amplitude in the steady state and recovery phase. Whitney U test, *** $P < 0.001$, ** $P < 0.01$, and * $P < 0.05$. th. LUT: thermal LUT; biot. TR: biotinylated transferrin; ctrl: control; and siR: siRNA. Scale bars: 5 μm in (A, B, D–G).

KO mice (Fig. 4K,L). This points to enhanced rates of GABAergic synaptic vesicle replenishment upon *Dnmt1* deletion. Already during depletion (10 Hz stimulation), IPSC amplitudes were significantly augmented in *Dnmt1*-deficient mice compared with WT, suggesting a shift in the baseline due to permanently improved replenishment (Fig. 4K,L). These data are coherent with the increased frequencies of mIPSCs detected in *Pvalb-Cre/tdTomato/Dnmt1 loxP2* mice (Fig. 1A–C) and suggest an elevated GABAergic transmission that might be caused by accelerated vesicle recycling after *Dnmt1* deletion.

Together, we here propose a novel role of DNMT1-dependent DNA methylation in modulating synaptic function by adjusting clathrin-mediated endocytosis. While DNMT1-mediated DNA methylation of endocytosis-related genes appears to act as a brake on vesicle recycling and presumably presynaptic transmission, TET-mediated actions seem to promote endocytosis-based processes.

Altered synaptic transmission is known to be implicated in TLE as well as neocortical epilepsies (Kapur 2008), and several studies suggest defective synaptic vesicle endocytosis as disease mechanism in epilepsy (Helbig et al. 2019). As changes in *Dnmt1* and *Dnmt3a* expression were observed in patients with TLE (reviewed in Henshall and Kobow 2015), we wondered whether the DNA methylation and gene-expression profiles of endocytosis-related genes identified as DNMT1 targets in the mouse model are affected in human hippocampal tissue of TLE

patients (clinical parameters of TLE patients are collected in Table S4). Indeed, we identified endocytosis-annotated target genes of DNMT1-dependent DNA methylation in mice that displayed a significant correlation between gene expression and seizure rate (Fig. 5A), as well as differentially methylated sites in TLE patients when comparing groups of high- versus low-seizure frequencies (Table S5). For *Wipf1*, we even identified four differentially methylated CpG sites in human TLE patients with an orthologous differentially methylated site in *Dnmt1*-deficient mice around the promoter region (Fig. 5B,C). Albeit not orthologous, we found differentially methylated sites for all other genes shown in Figure 5A in both, mice and human samples, which are presented in Table S6. In line with that, the endocytosis-related genes depicted in Figure 5A (except *AP2BP1*) display a significant correlation with DNMT1 expression levels in the patient samples (Table S7). Together, these findings propose another piece to the puzzle of how DNMT1-dependent DNA methylation acts on synapse-specific function, strongly supporting an implication in endocytosis regulation with potential relevance for the pathophysiology of epilepsy.

Discussion

Here we describe a novel function of DNMT1-dependent DNA methylation in adjusting clathrin-mediated endocytosis,

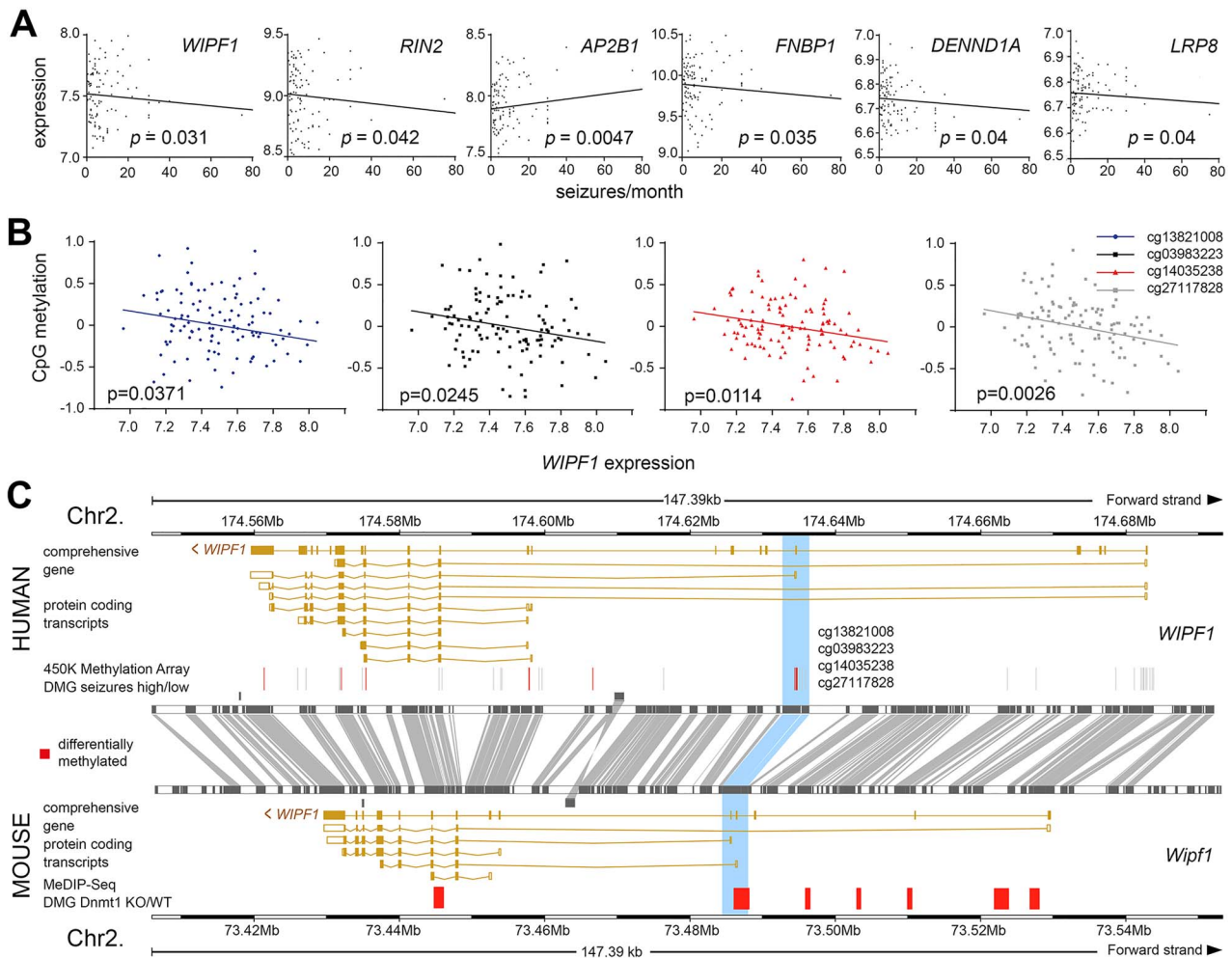


Figure 5. A correlation of endocytosis-related gene expression and seizure frequency is observed in hippocampal tissue of patients with TLE. (A) Gene expression correlation analysis for human data showing endocytosis-related genes, which are differentially expressed, as well as differentially methylated in both, the human and mouse dataset. (B) Correlation analysis for significantly altered CpG sites in the TSS of the *WIPF1* gene (positions shown in C) showing a negative correlation of methylation and expression level in TLE patients. (C) Orthologue analysis of the methylation profile (red marks) for *WIPF1* revealed similar differentially TSS methylation in the human as well as for the mouse dataset (light blue). Spearman correlation coefficient is shown in A and B. $N = 6$ mice per genotype were used for RNA- and MeDIP-Seq; WT: wild-type; KO: knockout; and TSS: transcription start site.

thereby modulating the synaptic transmission of cortical interneurons in the murine cerebral cortex.

DNMT-dependent DNA methylation is an epigenetic mechanism regulating gene expression during neuronal development, adult function, aging, and disease (Akbarian et al. 2013). DNMT1 and DNMT3A are the main DNA methyltransferases expressed in the developing and adult nervous system including glutamatergic and GABAergic neurons of the cerebral cortex (Feng and Fan 2009; Kadriu et al. 2012). The role of DNMT1 in neuronal development ranges from astrocytic gene suppression in cortical progenitors during neurogenesis (Fan et al. 2001) over the regulation of cell death and shape of migrating cortical interneurons (Pensold et al. 2017) to the control of survival and postmitotic maturation of excitatory cortical neurons (Hutnick et al. 2009).

Although the methylation of cytosines, often correlated with transcriptional repression (Wolffe 1998; Robertson 2002; Goll and Bestor 2005), is a chemically stable modification (Wu and Zhang 2017), active ways of DNA demethylation have been

described in postmitotic neurons. This includes TET-mediated iterative oxidation of 5mC to 5-hydroxymethylcytosine (5hmC), 5-formylcytosine (5fC), and 5-carboxylcytosine (5caC) followed by TDG-mediated excision of 5fC and 5caC coupled to base excision repair (Wu and Zhang 2010, 2014, 2017). In the adult central nervous system of mice and humans, 5hmC is present at high levels (Kriaucionis and Heintz 2009; Globisch et al. 2010; Lister et al. 2013) and enriched in gene bodies of differentiating and mature neurons (Lister et al. 2013; Hahn et al. 2014; Lister and Mukamel 2015). In addition to the function of 5hmC as intermediate in enzyme-catalyzed active DNA demethylation, there is evidence for a positive correlation of 5hmC with transcriptional level, which might be accomplished through crosstalk with histone modifications (Hahn et al. 2013; Sun et al. 2014). Together, this underlines the relevance of dynamic gene body DNA methylation for transcriptional control, which was already reported for neurons of the maturing nervous system (Lister et al. 2013; Benes 2015). Consistent with the

transcriptional potential of gene body methylation, we detected most DNA methylation changes in gene bodies after *Dnmt1* deletion in cortical interneurons (Fig. 2C,F).

In addition to aging and developmental processes, emerging evidence points to an important role of DNA methylation and demethylation in neuronal plasticity as well as learning and memory in the adult nervous system, mediated by active DNA demethylation and de novo methylation (Lister et al. 2013; Sweatt 2016). DNA methylation, which can be modulated by neuronal activity (Guo et al. 2011a), affects the expression of genes involved in functional plasticity and synaptic wiring (Halder et al. 2016). In differentiated glutamatergic cortical neurons, DNMT1-dependent DNA methylation was described to contribute to the regulation of synaptic scaling and plasticity (Feng et al. 2010; Meadows et al. 2015). Blocking DNMTs affected membrane excitability (Meadows et al. 2016) and changed excitatory synaptic transmission (Nelson et al. 2008).

In line with that, TET-mediated DNA demethylation controls long-lasting changes in synaptic function and behavior (reviewed in Sweatt (2016)). TET1 was reported to regulate expression of activity-regulated genes, synaptic plasticity, and memory extinction (Rudenko et al. 2013). TET3-mediated active DNA demethylation is implicated in the regulation of synaptic transmission and surface levels of GluR1 receptors in hippocampal neurons (Yu et al. 2015). Hence, dynamic DNA methylation seems to be crucial for neuronal function and plasticity. Consistently, our data indicate that DNMT1 influences the GABAergic transmission of *Pvalb*-expressing cortical interneurons.

PV-positive GABAergic interneurons perform crucial functions in the cerebral cortex orchestrating cortical oscillation and maintaining cortical network activity (Cardin et al. 2009; Sohal et al. 2009; Uhlhaas and Singer 2010; Isaacson and Scanziani 2011; Yizhar et al. 2011). Due to their relevance for working memory and cognition (Murray et al. 2015), dysfunctions of PV-interneurons in the prefrontal cortex had been linked to the pathophysiology of schizophrenia (Beasley and Reynolds 1997; Lewis et al. 2012). In this context, altered DNMT1-dependent gene regulation seems to contribute to the defects in the GABAergic system of schizophrenia patients (Costa et al. 2003; Veldic et al. 2004; Ruzicka et al. 2007).

Although we detected transcriptional changes for genes involved in synaptic function and excitability in *Dnmt1*-deficient cortical interneurons, a direct control of interneuron activity through canonical DNMT1 action by repressive DNA methylation of these genes in WT appeared unlikely. Many of these transcripts displayed reduced expression after *Dnmt1* deletion, and most of the observed transcriptional alterations did not correlate with respective changes in DNA methylation (Fig. 3). This could be explained by indirect effects caused by *Dnmt1* deletion. As DNMT1 was described to interact with histone-modifying complexes (Esteve et al. 2006; Vire et al. 2006; Ning et al. 2015), these transcriptional changes could be due to defects in DNMT1-dependent changes in histone modifications, which we previously observed in embryonic interneurons (Symmank et al. 2018). Indeed, histone modification-associated genes were altered in transcription in *Dnmt1*-deficient interneurons (Table S3), which could lead to indirect effects and which would point to noncanonical DNMT1 actions in WT interneurons that were not investigated here. Of the few synaptic activity-related genes that were indeed affected in both, expression and methylation, the majority displayed an increased methylation and reduced expression level in *Dnmt1*-deficient cells (Fig. 3B).

One possible explanation for the increased methylation upon *Dnmt1* deletion could be a compensatory DNA methylation-dependent transcriptional control by DNMT3a, which is likewise expressed at high levels in cortical interneurons (Tables S1 and S3; Kadriu et al. 2012), but which was not significantly altered in *Dnmt1*-deficient interneurons (Fig. S2). Hence, independent of its own transcriptional dysregulation DNMT3a could act differentially on methylation due to *Dnmt1* deletion, especially as diverse other genes related to DNA methylation and demethylation processes are changed in expression in *Dnmt1*-deficient cells (Table S3). Together, these alterations might have diverse effects on the DNA methylation level.

Moreover, apart from the conventional view that transcription factors do not interact with methylated DNA, emerging in vitro but also in vivo evidence exists for a new role of transcription factors acting as readers of DNA methylation, mediating methylation-dependent biological processes (Zhu et al. 2016). Hence, altered DNA methylation profiles resulting from *Dnmt1* deletion could lead to changes in binding motifs for certain transcription factors, which consequently could cause the observed changes in expression of synapse and activity-related genes (Fig. 3).

As numerous genes associated to the clathrin-mediated endocytosis pathway were upregulated in expression and reduced in methylation upon *Dnmt1* deletion (Fig. 2G–I), a direct regulation of endocytosis by canonical DNMT1 function through repressive DNA methylation in WT can be assumed. Supported by functional in vitro studies, our data emphasize that dynamic DNMT1-dependent DNA methylation is involved in modulating clathrin-mediated endocytosis.

Apart from maintaining cellular homeostasis clathrin-dependent endocytosis is crucially implicated in the regulation of synaptic function (Kuromi and Kidokoro 2005). In general, endocytosed cargo is either recycled back to the membrane via early endosomes, subjected to retrograde retrieval by the transport from endosomes to the trans-Golgi network or enters the endolysosomal degradation pathway (Huotari and Helenius 2011). Consistent with the relevance of endocytosis-dependent processes at the pre- and post-synapse for synaptic activity regulation (Maycox et al. 1992), we propose that DNA-methylation and demethylation events indirectly affect interneuron activity by modulating clathrin-mediated endocytosis. In support of this, *Tet1*-deletion had an opposite effect on clathrin-mediated endocytosis and the expression of *Wipf1* (Fig. 4D–I), an endocytosis-related gene. Moreover, TET-dependent control of glutamate receptor surface levels and trafficking was already described at the postsynapse (Yu et al. 2015; Sweatt 2016), to which endocytosis modulation could contribute.

At the presynaptic site, clathrin-mediated endocytosis together with bulk and ultrafast endocytosis replenish synaptic vesicles, which also affects neuronal activity (Smith et al. 2008; Cousin 2009; Park et al. 2016; Watanabe and Boucrot 2017). The increased concentrations of extracellular GABA and vesicle replenishment in conditional *Dnmt1*-deficient mice strongly suggest that DNMT1 is implicated in this process.

This hypothesis is supported by human brain sample analysis of patients suffering from TLE, a disease characterized by altered synaptic transmission (Kapur 2008). Moreover, changes in neuronal *Dnmt1* and *Dnmt3a* expression were observed in patients with TLE (reviewed in Henshall and Kobow (2015)) and a recent study proposed defective synaptic vesicle endocytosis as disease mechanism in epilepsy (Helbig et al. 2019). Consistently, we identified differential methylation of

endocytosis-annotated DNMT1 target genes that displayed a significant correlation between gene expression and seizure rate (Fig. 5A) in TLE patients with high- versus low-seizure frequencies (Table S5). Moreover, five of these six genes correlate in with DNMT1 expression in the TLE samples (Table S7). These observations support an implication of DNA methylation-dependent endocytosis regulation in the pathophysiology of TLE. As the analyzed hippocampal tissue was composed of both, inhibitory as well as excitatory neurons, it is conceivable that DNA methylation-dependent synaptic function regulation through endocytosis modulation is not restricted to inhibitory cortical interneurons. In support of this, DNMT1-dependent effects on endocytosis were also seen in N2a and CB cell culture models (Fig. S4).

Neuronal activity was described to alter gene expression through dynamic DNA methylation (Nelson et al. 2008; Sharma et al. 2008; Guo et al. 2011a). Hence, the fine tuning of endocytosis by DNA methylation and in turn synaptic transmission could be part of an adaptive regulatory network with potential relevance for synaptic plasticity. The outlasting time scale needed for neuronal activity regulation by DNA methylation-modulated endocytosis triggered by activity would support a possible implication in metaplasticity, which entails a change of a neuron's current physiological or biochemical state and the ability for synaptic plasticity dependent on its history (Abraham 2008). Hence, in addition to the transcriptional control of plasticity-related genes (Halder et al. 2016), dynamic DNA methylation could contribute to synaptic plasticity and metaplasticity by modulating endocytic processes.

Supplementary Material

Supplementary material can be found at Cerebral Cortex online.

Funding

The Deutsche Forschungsgemeinschaft (DFG, German Research Foundation) (368482240/GRK2416 and ZI 1224/4-1); the IZKF Jena to G.Z.B.; and the ESF (2016 FGR 0024) to C.A.H.

Notes

We thank Susanne Luthin and Fabian Ludewig for excellent technical assistance. We further thank Dr. Michael Reichelt danken from the Max Planck Institute for Chemical Ecology, Department for Biochemistry, Jena, for the HPLC measurements.

References

- Abraham WC. 2008. Metaplasticity: tuning synapses and networks for plasticity. *Nat Rev Neurosci.* 9(5):387. doi: 10.1038/nrn2356.
- Akbadian S, Beeri MS, Haroutunian V. 2013. Epigenetic determinants of healthy and diseased brain aging and cognition. *JAMA Neurol.*
- Akhtar N, Hotchin NA. 2001. RAC1 regulates adherens junctions through endocytosis of E-cadherin. *Mol Biol Cell.* 12(4):847–862. Retrieved from: <https://www.ncbi.nlm.nih.gov/pmc/articles/PMC32271/pdf/mk000847.pdf>.
- Asgatay S, Champion C, Marloie G, Drujon T, Senamaud-Beaufort C, Ceccaldi A, Guianvarc'h D. 2014. Synthesis and evaluation of analogues of N-phthaloyl-L-tryptophan (RG108) as inhibitors of DNA methyltransferase 1. *J Med Chem.* 57(2):421–434. doi: 10.1021/jm401419p.
- Bandler RC, Mayer C, Fishell G. 2017. Cortical interneuron specification: the juncture of genes, time and geometry. *Curr Opin Neurobiol.* 42:17–24. doi: 10.1016/j.conb.2016.10.003.
- Beasley CL, Reynolds GP. 1997. Parvalbumin-immunoreactive neurons are reduced in the prefrontal cortex of schizophrenics. *Schizophr Res.* 24(3):349–355.
- Benes FM. 2015. The GABA system in schizophrenia: cells, molecules and microcircuitry. *Schizophr Res.* 167(1–3):1–3. doi: 10.1016/j.schres.2015.07.017.
- Bestor TH. 2000. The DNA methyltransferases of mammals. *Hum Mol Genet.* 9(16):2395–2402.
- Bouron A. 2001. Modulation of spontaneous quantal release of neurotransmitters in the hippocampus. *Prog Neurobiol.* 63(6):613–635.
- Bredt DS, Nicoll RA. 2003. AMPA receptor trafficking at excitatory synapses. *Neuron.* 40(2):361–379.
- Brewer GJ. 1997. Isolation and culture of adult rat hippocampal neurons. *J Neurosci Methods.* 71(2):143–155. Retrieved from <http://www.ncbi.nlm.nih.gov/pubmed/9128149>, http://ac.els-cdn.com/S0165027096001367/1-s2.0-S0165027096001367-main.pdf?_tid=add2c8c4-6344-11e4-93b5-00000aacb360&acdnat=1415010915_68040cff142f7d0ae25e63d57963db43.
- Brewer GJ, Torricelli JR. 2007. Isolation and culture of adult neurons and neurospheres. *Nat Protoc.* 2(6):1490–1498. doi: 10.1038/nprot.2007.207.
- Brueckner B, Garcia Boy R, Siedlecki P, Musch T, Kliem HC, Zielenkiewicz P, Lyko F. 2005. Epigenetic reactivation of tumor suppressor genes by a novel small-molecule inhibitor of human DNA methyltransferases. *Cancer Res.* 65(14):6305–6311. doi: 10.1158/0008-5472.CAN-04-2957.
- Buzsaki G, Wang XJ. 2012. Mechanisms of gamma oscillations. *Annu Rev Neurosci.* 35:203–225. doi: 10.1146/annurev-neuro-062111-150444.
- Cajigas JJ, Will T, Schuman EM. 2010. Protein homeostasis and synaptic plasticity. *EMBO J.* 29(16):2746–2752. doi: 10.1038/emboj.2010.173.
- Cardin JA, Carlen M, Meletis K, Knoblich U, Zhang F, Deisseroth K, Moore CI. 2009. Driving fast-spiking cells induces gamma rhythm and controls sensory responses. *Nature.* 459(7247):663–667. doi: 10.1038/nature08002 [doi].
- Cosker KE, Segal RA. 2014. Neuronal signaling through endocytosis. *Cold Spring Harb Perspect Biol.* 6(2). doi: 10.1101/cshperspect.a020669.
- Costa E, Grayson DR, Guidotti A. 2003. Epigenetic downregulation of GABAergic function in schizophrenia: potential for pharmacological intervention? *Mol Interv.* 3(4):220–229. doi: 10.1124/mi.3.4.220.
- Cousin MA. 2009. Activity-dependent bulk synaptic vesicle endocytosis—a fast, high capacity membrane retrieval mechanism. *Mol Neurobiol.* 39(3):185–189. doi: 10.1007/s12035-009-8062-3.
- Dobin A, Davis CA, Schlesinger F, Drenkow J, Zaleski C, Jha S, Gingeras TR. 2013. STAR: ultrafast universal RNA-seq aligner. *Bioinformatics.* 29(1):15–21. doi: 10.1093/bioinformatics/bts635.
- Druga R. 2009. Neocortical inhibitory system. *Folia Biol (Praha).* 55(6):201–217.
- Eide L, McMurray CT. 2005. Culture of adult mouse neurons. *BioTechniques.* 38(1):99–104. Retrieved from <http://www.ncbi.nlm.nih.gov/pubmed/15679091>.
- Esteve PO, Chin HG, Smallwood A, Feehery GR, Gangisetty O, Karpf AR, Pradhan S. 2006. Direct interaction between

- DNMT1 and G9a coordinates DNA and histone methylation during replication. *Genes Dev.* 20(22):3089–3103. doi: [10.1101/gad.1463706](https://doi.org/10.1101/gad.1463706).
- Fan G, Beard C, Chen RZ, Csankovszki G, Sun Y, Siniaia M, Jaenisch R. 2001. DNA hypomethylation perturbs the function and survival of CNS neurons in postnatal animals. *J Neurosci.* 21(3):788–797.
- Feng J, Fan G. 2009. The role of DNA methylation in the central nervous system and neuropsychiatric disorders. *Int Rev Neurobiol.* 89:67–84. doi: [10.1016/S0074-7742\(09\)89004-1](https://doi.org/10.1016/S0074-7742(09)89004-1).
- Feng J, Zhou Y, Campbell SL, Le T, Li E, Sweatt JD, Fan G. 2010. Dnmt1 and Dnmt3a maintain DNA methylation and regulate synaptic function in adult forebrain neurons. *Nat Neurosci.* 13(4):423–430. doi: [10.1038/nn.2514](https://doi.org/10.1038/nn.2514).
- Ferguson SM, Brasnjo G, Hayashi M, Wolfel M, Collesi C, Giovedi S, De Camilli P. 2007. A selective activity-dependent requirement for dynamin 1 in synaptic vesicle endocytosis. *Science.* 316(5824):570–574. doi: [10.1126/science.1140621](https://doi.org/10.1126/science.1140621).
- Fries P. 2009. Neuronal gamma-band synchronization as a fundamental process in cortical computation. *Annu Rev Neurosci.* 32:209–224. doi: [10.1146/annurev.neuro.051508.135603](https://doi.org/10.1146/annurev.neuro.051508.135603).
- Galarreta M, Hestrin S. 1998. Frequency-dependent synaptic depression and the balance of excitation and inhibition in the neocortex. *Nat Neurosci.* 1(7):587–594. doi: [10.1038/2882](https://doi.org/10.1038/2882).
- Globisch D, Munzel M, Muller M, Michalakakis S, Wagner M, Koch S, Carell T. 2010. Tissue distribution of 5-hydroxymethylcytosine and search for active demethylation intermediates. *PLoS One.* 5(12):e15367. doi: [10.1371/journal.pone.0015367](https://doi.org/10.1371/journal.pone.0015367).
- Goll MG, Bestor TH. 2005. Eukaryotic cytosine methyltransferases. *Annu Rev Biochem.* 74:481–514. doi: [10.1146/annurev.biochem.74.010904.153721](https://doi.org/10.1146/annurev.biochem.74.010904.153721).
- Guo JU, Ma DK, Mo H, Ball MP, Jang MH, Bonaguidi MA, Song H. 2011a. Neuronal activity modifies the DNA methylation landscape in the adult brain. *Nat Neurosci.* 14(10):1345–1351. doi: [10.1038/nn.2900](https://doi.org/10.1038/nn.2900).
- Guo JU, Su Y, Shin JH, Shin J, Li H, Xie B, Fan G. 2014. Distribution, recognition and regulation of non-CpG methylation in the adult mammalian. *Brain.* 17(2):215–222. doi: [10.1038/nn.3607](https://doi.org/10.1038/nn.3607).
- Guo JU, Su Y, Zhong C, Ming GL, Song H. 2011b. Hydroxylation of 5-methylcytosine by TET1 promotes active DNA demethylation in the adult brain. *Cell.* 145(3):423–434. doi: [10.1016/j.cell.2011.03.022](https://doi.org/10.1016/j.cell.2011.03.022).
- Hahn MA, Qiu R, Wu X, Li AX, Zhang H, Wang J, Lu Q. 2013. Dynamics of 5-hydroxymethylcytosine and chromatin marks in mammalian neurogenesis. *Cell Rep.* 3(2):291–300. doi: [10.1016/j.celrep.2013.01.011](https://doi.org/10.1016/j.celrep.2013.01.011).
- Hahn MA, Szabo PE, Pfeifer GP. 2014. 5-Hydroxymethylcytosine: a stable or transient DNA modification? *Genomics.* 104(5):314–323. doi: [10.1016/j.ygeno.2014.08.015](https://doi.org/10.1016/j.ygeno.2014.08.015).
- Halder R, Hennion M, Vidal RO, Shomroni O, Rahman RU, Rajput A, Bonn S. 2016. DNA methylation changes in plasticity genes accompany the formation and maintenance of memory. *Nat Neurosci.* 19(1):102–110. doi: [10.1038/nn.4194](https://doi.org/10.1038/nn.4194).
- Helbig I, Lopez-Hernandez T, Shor O, Galer P, Ganesan S, Pendziwiat M, Weber YG. 2019. A recurrent missense variant in AP2M1 impairs Clathrin-mediated endocytosis and causes developmental and epileptic encephalopathy. *Am J Hum Genet.* doi: [10.1016/j.ajhg.2019.04.001](https://doi.org/10.1016/j.ajhg.2019.04.001).
- Hensch TK. 2005. Critical period plasticity in local cortical circuits. *Nat Rev Neurosci.* 6(11):877–888. doi: [10.1038/nrn1787](https://doi.org/10.1038/nrn1787).
- Hensch TK, Fagioli M. 2005. Excitatory-inhibitory balance and critical period plasticity in developing visual cortex. *Prog Brain Res.* 147:115–124. doi: [10.1016/S0079-6123\(04\)47009-5](https://doi.org/10.1016/S0079-6123(04)47009-5).
- Henshall DC, Kobow K. 2015. Epigenetics and epilepsy. *Cold Spring Harb Perspect Med.* 5(12). doi: [10.1101/cshperspect.a022731](https://doi.org/10.1101/cshperspect.a022731).
- Hippenmeyer S, Vrieseling E, Sigrist M, Portmann T, Laengle C, Ladle DR, Arber S. 2005. A developmental switch in the response of DRG neurons to ETS transcription factor signaling. *PLoS Biol.* 3(5):e159. doi: [10.1371/journal.pbio.0030159](https://doi.org/10.1371/journal.pbio.0030159).
- Huang HS, Akbarian S. 2007. GAD1 mRNA expression and DNA methylation in prefrontal cortex of subjects with schizophrenia. *PLoS One.* 2(8):e809. doi: [10.1371/journal.pone.0000809](https://doi.org/10.1371/journal.pone.0000809).
- Huotari J, Helenius A. 2011. Endosome maturation. *EMBO J.* 30(17):3481–3500. doi: [10.1038/emboj.2011.286](https://doi.org/10.1038/emboj.2011.286).
- Hutnick LK, Golshani P, Namihira M, Xue Z, Matynia A, Yang XW, Fan G. 2009. DNA hypomethylation restricted to the murine forebrain induces cortical degeneration and impairs postnatal neuronal maturation. *Hum Mol Genet.* 18(15):2875–2888. doi: [10.1093/hmg/ddp222](https://doi.org/10.1093/hmg/ddp222).
- Isaacson JS, Scanziani M. 2011. How inhibition shapes cortical activity. *Neuron.* 72(2):231–243. doi: [10.1016/j.neuron.2011.09.027](https://doi.org/10.1016/j.neuron.2011.09.027).
- Ito S, Shen L, Dai Q, Wu SC, Collins LB, Swenberg JA, Zhang Y. 2011. Tet proteins can convert 5-methylcytosine to 5-formylcytosine and 5-carboxylcytosine. *Science.* 333(6047):1300–1303. doi: [10.1126/science.1210597](https://doi.org/10.1126/science.1210597).
- Jackson-Grusby L, Beard C, Possemato R, Tudor M, Fambrough D, Csankovszki G, Jaenisch R. 2001. Loss of genomic methylation causes p53-dependent apoptosis and epigenetic deregulation. *Nat Genet.* 27(1):31–39. doi: [10.1038/83730](https://doi.org/10.1038/83730).
- Johnson MR, Behmoaras J, Bottolo L, Krishnan ML, Pernhorst K, Santoscoy PLM, Petretto E. 2015. Systems genetics identifies Sestrin 3 as a regulator of a proconvulsant gene network in human epileptic hippocampus. *Nat Commun.* 6:6031. doi: [10.1038/ncomms7031](https://doi.org/10.1038/ncomms7031).
- Kaas GA, Zhong C, Eason DE, Ross DL, Vachhani RV, Ming GL, Sweatt JD. 2013. TET1 controls CNS 5-methylcytosine hydroxylation, active DNA demethylation, gene transcription and memory formation. *Neuron.* 79(6):1086–1093. doi: [10.1016/j.neuron.2013.08.032](https://doi.org/10.1016/j.neuron.2013.08.032).
- Kadriu B, Guidotti A, Chen Y, Grayson DR. 2012. DNA methyltransferases1 (DNMT1) and 3a (DNMT3a) colocalize with GAD67-positive neurons in the GAD67-GFP mouse brain. *J Comp Neurol.* 520(9):1951–1964. doi: [10.1002/cne.23020](https://doi.org/10.1002/cne.23020).
- Kapur J. 2008. Is epilepsy a disease of synaptic transmission? *Epilepsy Curr.* 8(5):139–141. doi: [10.1111/j.1535-7511.2008.00271.x](https://doi.org/10.1111/j.1535-7511.2008.00271.x).
- Kelsom C, Lu W. 2013. Development and specification of GABAergic cortical interneurons. *Cell Biosci.* 3(1):19. doi: [10.1186/2045-3701-3-19](https://doi.org/10.1186/2045-3701-3-19).
- Kohli RM, Zhang Y. 2013. TET enzymes, TDG and the dynamics of DNA demethylation. *Nature.* 502(7472):472–479. doi: [10.1038/nature12750](https://doi.org/10.1038/nature12750).
- Kral T, Clusmann H, Urbach J, Schramm J, Elger CE, Kurthen M, Grunwald T. 2002. Preoperative evaluation for epilepsy surgery (Bonn algorithm). *Zentralbl Neurochir.* 63(3):106–110. doi: [10.1055/s-2002-35826](https://doi.org/10.1055/s-2002-35826).
- Kriaucionis S, Heintz N. 2009. The nuclear DNA base 5-hydroxymethylcytosine is present in Purkinje neurons and the brain. *Science.* 324(5929):929–930. doi: [10.1126/science.1169786](https://doi.org/10.1126/science.1169786).
- Kuromi H, Kidokoro Y. 2005. Exocytosis and endocytosis of synaptic vesicles and functional roles of vesicle pools: lessons from the drosophila neuromuscular junction. *Neuroscientist.* 11(2):138–147. doi: [10.1177/1073858404271679](https://doi.org/10.1177/1073858404271679).

- Letzkus JJ, Wolff SB, Luthi A. 2015. Disinhibition, a circuit mechanism for associative learning and memory. *Neuron*. 88(2):264–276. doi: [10.1016/j.neuron.2015.09.024](https://doi.org/10.1016/j.neuron.2015.09.024).
- Levenson JM, Roth TL, Lubin FD, Miller CA, Huang IC, Desai P, Sweatt JD. 2006. Evidence that DNA (cytosine-5) methyltransferase regulates synaptic plasticity in the hippocampus. *J Biol Chem*. 281(23):15763–15773. doi: [10.1074/jbc.M511767200](https://doi.org/10.1074/jbc.M511767200).
- Lewis DA, Curley AA, Glausier JR, Volk DW. 2012. Cortical parvalbumin interneurons and cognitive dysfunction in schizophrenia. *Trends Neurosci*. 35(1):57–67. doi: [10.1016/j.tins.2011.10.004](https://doi.org/10.1016/j.tins.2011.10.004).
- Li X, Wei W, Zhao QY, Widagdo J, Baker-Andresen D, Flavell CR, Bredy TW. 2014. Neocortical Tet3-mediated accumulation of 5-hydroxymethylcytosine promotes rapid behavioral adaptation. *Proc Natl Acad Sci U S A*. 111(19):7120–7125. doi: [10.1073/pnas.1318906111](https://doi.org/10.1073/pnas.1318906111).
- Liebmann L, Karst H, Joels M. 2009. Effects of corticosterone and the beta-agonist isoproterenol on glutamate receptor-mediated synaptic currents in the rat basolateral amygdala. *Eur J Neurosci*. 30(5):800–807. doi: [10.1111/j.1460-9568.2009.06882.x](https://doi.org/10.1111/j.1460-9568.2009.06882.x).
- Lienhard M, Grimm C, Morkel M, Herwig R, Chavez L. 2014. MEDIPS: genome-wide differential coverage analysis of sequencing data derived from DNA enrichment experiments. *Bioinformatics*. 30(2):284–286. doi: [10.1093/bioinformatics/btt650](https://doi.org/10.1093/bioinformatics/btt650).
- Lister R, Mukamel EA. 2015. Turning over DNA methylation in the mind. *Front Neurosci*. 9:252. doi: [10.3389/fnins.2015.00252](https://doi.org/10.3389/fnins.2015.00252).
- Lister R, Mukamel EA, Nery JR, Urich M, Puddifoot CA, Johnson ND, Ecker JR. 2013. Global epigenomic reconfiguration during mammalian brain development. *Science*. 341(6146):1237905. doi: [10.1126/science.1237905](https://doi.org/10.1126/science.1237905).
- Lodato S, Arlotta P. 2015. Generating neuronal diversity in the mammalian cerebral cortex. *Annu Rev Cell Dev Biol*. 31:699–720. doi: [10.1146/annurev-cellbio-100814-125353](https://doi.org/10.1146/annurev-cellbio-100814-125353).
- Love MI, Huber W, Anders S. 2014. Moderated estimation of fold change and dispersion for RNA-seq data with DESeq2. *Genome Biol*. 15(12):550. doi: [10.1186/s13059-014-0550-8](https://doi.org/10.1186/s13059-014-0550-8).
- Luo W, Brouwer C. 2013. Pathview: an R/bioconductor package for pathway-based data integration and visualization. *Bioinformatics*. 29(14):1830–1831. doi: [10.1093/bioinformatics/btt285](https://doi.org/10.1093/bioinformatics/btt285).
- Madisen L, Zwingman TA, Sunkin SM, Oh SW, Zariwala HA, Gu H, Zeng H. 2010. A robust and high-throughput Cre reporting and characterization system for the whole mouse brain. *Nat Neurosci*. 13(1):133–140. doi: [10.1038/nn.2467](https://doi.org/10.1038/nn.2467).
- Malinow R, Malenka RC. 2002. AMPA receptor trafficking and synaptic plasticity. *Annu Rev Neurosci*. 25:103–126. doi: [10.1146/annurev.neuro.25.112701.142758](https://doi.org/10.1146/annurev.neuro.25.112701.142758).
- Marin MP, Esteban-Pretel G, Ponsoda X, Romero AM, Ballestin R, Lopez C, Renau-Piqueras J. 2010. Endocytosis in cultured neurons is altered by chronic alcohol exposure. *Toxicol Sci*. 115(1):202–213. doi: [10.1093/toxsci/kfq040](https://doi.org/10.1093/toxsci/kfq040).
- Marin O. 2012. Interneuron dysfunction in psychiatric disorders. *Nat Rev Neurosci*. 13(2):107–120. doi: [10.1038/nrn3155](https://doi.org/10.1038/nrn3155).
- Matrisciano F, Tueting P, Dalal I, Kadriu B, Grayson DR, Davis JM, Guidotti A. 2013. Epigenetic modifications of GABAergic interneurons are associated with the schizophrenia-like phenotype induced by prenatal stress in mice. *Neuropharmacology*. 68:184–194. doi: [10.1016/j.neuropharm.2012.04.013](https://doi.org/10.1016/j.neuropharm.2012.04.013).
- Maycox PR, Link E, Reetz A, Morris SA, Jahn R. 1992. Clathrin-coated vesicles in nervous tissue are involved primarily in synaptic vesicle recycling. *J Cell Biol*. 118(6):1379–1388.
- Meadows JP, Guzman-Karlsson MC, Phillips S, Brown JA, Strange SK, Sweatt JD, Hablitz JJ. 2016. Dynamic DNA methylation regulates neuronal intrinsic membrane excitability. *Sci Signal*. 9(442):ra83. doi: [10.1126/scisignal.aaf5642](https://doi.org/10.1126/scisignal.aaf5642).
- Meadows JP, Guzman-Karlsson MC, Phillips S, Holleman C, Posey JL, Day JJ, Sweatt JD. 2015. DNA methylation regulates neuronal glutamatergic synaptic scaling. *Sci Signal*. 8(382):ra61. doi: [10.1126/scisignal.aab0715](https://doi.org/10.1126/scisignal.aab0715).
- Morris MJ, Adachi M, Na ES, Monteggia LM. 2014. Selective role for DNMT3a in learning and memory. *Neurobiol Learn Mem*. 115:30–37. doi: [10.1016/j.nlm.2014.06.005](https://doi.org/10.1016/j.nlm.2014.06.005).
- Morris MJ, Na ES, Autry AE, Monteggia LM. 2016. Impact of DNMT1 and DNMT3a forebrain knockout on depressive- and anxiety like behavior in mice. *Neurobiol Learn Mem*. 135:139–145. doi: [10.1016/j.nlm.2016.08.012](https://doi.org/10.1016/j.nlm.2016.08.012).
- Murray AJ, Woloszynowska-Fraser MU, Ansel-Bollepalli L, Cole KL, Foggetti A, Crouch B, Wulff P. 2015. Parvalbumin-positive interneurons of the prefrontal cortex support working memory and cognitive flexibility. *Sci Rep*. 5:16778. doi: [10.1038/srep16778](https://doi.org/10.1038/srep16778).
- Nelson ED, Kavalali ET, Monteggia LM. 2008. Activity-dependent suppression of miniature neurotransmission through the regulation of DNA methylation. *J Neurosci*. 28(2):395–406. doi: [10.1523/jneurosci.3796-07.2008](https://doi.org/10.1523/jneurosci.3796-07.2008).
- Ning X, Shi Z, Liu X, Zhang A, Han L, Jiang K, Zhang Q. 2015. DNMT1 and EZH2 mediated methylation silences the microRNA-200b/a/429 gene and promotes tumor progression. *Cancer Lett*. 359(2):198–205. doi: [10.1016/j.canlet.2015.01.005](https://doi.org/10.1016/j.canlet.2015.01.005).
- Park J, Cho OY, Kim JA, Chang S. 2016. Endosome-mediated endocytic mechanism replenishes the majority of synaptic vesicles at mature CNS synapses in an activity-dependent manner. *Sci Rep*. 6:31807. doi: [10.1038/srep31807](https://doi.org/10.1038/srep31807).
- Parton RG, Dotti CG. 1993. Cell biology of neuronal endocytosis. *J Neurosci Res*. 36(1):1–9. doi: [10.1002/jnr.490360102](https://doi.org/10.1002/jnr.490360102).
- Pensold D, Symmank J, Hahn A, Lingner T, Salinas-Riester G, Downie BR, Zimmer G. 2017. The DNA methyltransferase 1 (DNMT1) controls the shape and dynamics of migrating POA-derived interneurons fated for the murine cerebral cortex. *Cereb Cortex*. 27(12):5696–5714. doi: [10.1093/cercor/bhw341](https://doi.org/10.1093/cercor/bhw341).
- Robertson KD. 2002. DNA methylation and chromatin-unraveling the tangled web. *Oncogene*. 21(35):5361–5379. doi: [10.1038/sj.onc.1205609](https://doi.org/10.1038/sj.onc.1205609).
- Rudenko A, Dawlaty MM, Seo J, Cheng AW, Meng J, Le T, Tsai LH. 2013. Tet1 is critical for neuronal activity-regulated gene expression and memory extinction. *Neuron*. 79(6):1109–1122. doi: [10.1016/j.neuron.2013.08.003](https://doi.org/10.1016/j.neuron.2013.08.003).
- Ruzicka WB, Zhubi A, Veldic M, Grayson DR, Costa E, Guidotti A. 2007. Selective epigenetic alteration of layer I GABAergic neurons isolated from prefrontal cortex of schizophrenia patients using laser-assisted microdissection. *Mol Psychiatry*. 12(4):385–397. doi: [10.1038/sj.mp.4001954](https://doi.org/10.1038/sj.mp.4001954).
- Sananbenesi F, Fischer A. 2009. The epigenetic bottleneck of neurodegenerative and psychiatric diseases. *Biol Chem*. 390(11):1145–1153. doi: [10.1515/BC.2009.131](https://doi.org/10.1515/BC.2009.131).
- Saradalekshmi KR, Neetha NV, Sathyan S, Nair IV, Nair CM, Banerjee M. 2014. DNA methyl transferase (DNMT) gene polymorphisms could be a primary event in epigenetic susceptibility to schizophrenia. *PLoS One*. 9(5):e98182. doi: [10.1371/journal.pone.0098182](https://doi.org/10.1371/journal.pone.0098182).

- Saxena A, Wagatsuma A, Noro Y, Kuji T, Asaka-Oba A, Watahiki A, Carninci P. 2012. Trehalose-enhanced isolation of neuronal sub-types from adult mouse brain. *BioTechniques*. 52(6):381–385. doi: [10.2144/0000113878](https://doi.org/10.2144/0000113878).
- Schindelin J, Arganda-Carreras I, Frise E, Kaynig V, Longair M, Pietzsch T, Cardona A. 2012. Fiji: an open-source platform for biological-image analysis. *Nat Methods*. 9(7):676–682. doi: [10.1038/nmeth.2019](https://doi.org/10.1038/nmeth.2019).
- Schneggenburger R, Meyer AC, Neher E. 1999. Released fraction and total size of a pool of immediately available transmitter quanta at a calyx synapse. *Neuron*. 23(2):399–409.
- Schulz H, Ruppert AK, Herms S, Wolf C, Mirza-Schreiber N, Stegle O, Cichon S. 2017. Genome-wide mapping of genetic determinants influencing DNA methylation and gene expression in human hippocampus. *Nat Commun*. 8(1):1511. doi: [10.1038/s41467-017-01818-4](https://doi.org/10.1038/s41467-017-01818-4).
- Sharma RP, Tun N, Grayson DR. 2008. Depolarization induces downregulation of DNMT1 and DNMT3a in primary cortical cultures. *Epigenetics*. 3(2):74–80.
- Smith SM, Renden R, von Gersdorff H. 2008. Synaptic vesicle endocytosis: fast and slow modes of membrane retrieval. *Trends Neurosci*. 31(11):559–568. doi: [10.1016/j.tins.2008.08.005](https://doi.org/10.1016/j.tins.2008.08.005).
- Sohal VS, Zhang F, Yizhar O, Deisseroth K. 2009. Parvalbumin neurons and gamma rhythms enhance cortical circuit performance. *Nature*. 459(7247):698–702. doi: [10.1038/nature07991](https://doi.org/10.1038/nature07991).
- Sun W, Zang L, Shu Q, Li X. 2014. From development to diseases: the role of 5hmC in brain. *Genomics*. doi:[10.1016/j.ygeno.2014.08.021](https://doi.org/10.1016/j.ygeno.2014.08.021).
- Sweatt JD. 2016. Dynamic DNA methylation controls glutamate receptor trafficking and synaptic scaling. *J Neurochem*. 137(3):312–330. doi: [10.1111/jnc.13564](https://doi.org/10.1111/jnc.13564).
- Sweatt JD. 2017. Layered-up regulation in the developing brain. *Nature*. 551(7681):448–449. doi: [10.1038/d41586-017-07269-7](https://doi.org/10.1038/d41586-017-07269-7).
- Symmank J, Bayer C, Schmidt C, Hahn A, Pensold D, Zimmer-Bensch G. 2018. DNMT1 modulates interneuron morphology by regulating Pak6 expression through crosstalk with histone modifications. *Epigenetics*. 13(5):536–556. doi: [10.1080/15592294.2018.1475980](https://doi.org/10.1080/15592294.2018.1475980).
- Symmank J, Zimmer G. 2017. Regulation of neuronal survival by DNA methyltransferases. *Neural Regen Res*. 12(11):1768–1775. doi: [10.4103/1673-5374.219027](https://doi.org/10.4103/1673-5374.219027).
- Turrigiano GG. 2008. The self-tuning neuron: synaptic scaling of excitatory synapses. *Cell*. 135(3):422–435. doi:[10.1016/j.cell.2008.10.008](https://doi.org/10.1016/j.cell.2008.10.008).
- Uhlhaas PJ, Singer W. 2010. Abnormal neural oscillations and synchrony in schizophrenia. *Nat Rev Neurosci*. 11(2):100–113. doi: [10.1038/nrn2774](https://doi.org/10.1038/nrn2774).
- van Loo KM, Schaub C, Pitsch J, Kulbida R, Opitz T, Ekstein D, Becker AJ. 2015. Zinc regulates a key transcriptional pathway for epileptogenesis via metal-regulatory transcription factor 1. *Nat Commun*. 6:8688. doi: [10.1038/ncomms9688](https://doi.org/10.1038/ncomms9688).
- Veldic M, Caruncho HJ, Liu WS, Davis J, Satta R, Grayson DR, Costa E. 2004. DNA-methyltransferase 1 mRNA is selectively overexpressed in telencephalic GABAergic interneurons of schizophrenia brains. *Proc Natl Acad Sci U S A*. 101(1):348–353. doi: [10.1073/pnas.2637013100](https://doi.org/10.1073/pnas.2637013100).
- Vercauteren D, Vandenbroucke RE, Jones AT, Rejman J, Demeester J, De Smedt SC, Braeckmans K. 2010. The use of inhibitors to study endocytic pathways of gene carriers: optimization and pitfalls. *Mol Ther*. 18(3):561–569. doi: [10.1038/mt.2009.281](https://doi.org/10.1038/mt.2009.281).
- Vire E, Brenner C, Deplus R, Blanchon L, Fraga M, Didelot C, Fuks F. 2006. The polycomb group protein EZH2 directly controls DNA methylation. *Nature*. 439(7078):871–874. doi: [10.1038/nature04431](https://doi.org/10.1038/nature04431).
- Watanabe S, Boucrot E. 2017. Fast and ultrafast endocytosis. *Curr Opin Cell Biol*. 47:64–71. doi: [10.1016/j.ceb.2017.02.013](https://doi.org/10.1016/j.ceb.2017.02.013).
- Wolffe AP. 1998. Packaging principle: how DNA methylation and histone acetylation control the transcriptional activity of chromatin. *J Exp Zool*. 282(1–2):239–244.
- Wu H, Zhang Y. 2014. Reversing DNA methylation: mechanisms, genomics and biological functions. *Cell*. 156(1–2):45–68. doi: [10.1016/j.cell.2013.12.019](https://doi.org/10.1016/j.cell.2013.12.019).
- Wu SC, Zhang Y. 2010. Active DNA demethylation: many roads lead to Rome. *Nat Rev Mol Cell Biol*. 11(9):607–620. doi: [10.1038/nrm2950](https://doi.org/10.1038/nrm2950).
- Wu X, Inoue A, Suzuki T, Zhang Y. 2017. Simultaneous mapping of active DNA demethylation and sister chromatid exchange in single cells. *Genes Dev*. 31(5):511–523. doi: [10.1101/gad.294843.116](https://doi.org/10.1101/gad.294843.116).
- Wu X, Zhang Y. 2017. TET-mediated active DNA demethylation: mechanism, function and beyond. *Nat Rev Genet*. 18(9):517–534. doi: [10.1038/nrg.2017.33](https://doi.org/10.1038/nrg.2017.33).
- Xie S, Bahl K, Reinecke JB, Hammond GR, Naslavsky N, Caplan S. 2016. The endocytic recycling compartment maintains cargo segregation acquired upon exit from the sorting endosome. *Mol Biol Cell*. 27(1):108–126. doi: [10.1091/mbc.E15-07-0514](https://doi.org/10.1091/mbc.E15-07-0514).
- Yizhar O, Fenno LE, Prigge M, Schneider F, Davidson TJ, O’Shea DJ, Deisseroth K. 2011. Neocortical excitation/inhibition balance in information processing and social dysfunction. *Nature*. 477(7363):171–178. doi: [10.1038/nature10360](https://doi.org/10.1038/nature10360).
- Yu H, Su Y, Shin J, Zhong C, Guo JU. 2015. Tet3 regulates synaptic transmission and homeostatic plasticity via DNA oxidation and repair. *Nat Neurosci*. 18(6):836–843. doi: [10.1038/nn.4008](https://doi.org/10.1038/nn.4008).
- Zhu H, Wang G, Qian J. 2016. Transcription factors as readers and effectors of DNA methylation. *Nat Rev Genet*. 17(9):551–565. doi: [10.1038/nrg.2016.83](https://doi.org/10.1038/nrg.2016.83).
- Zimmer G, Rudolph J, Landmann J, Gerstmann K, Steinecke A, Gampe C, Bolz J. 2011. Bidirectional ephrinB3/EphA4 signaling mediates the segregation of MGE and POA derived interneurons in the deep and superficial migratory stream. *J Neurosci*. 31(50): 18364–18380.